
IMPACTS OF CLIMATE CHANGE ON FLOW COMPOSITION USING A MODEL TAILORED TO RUNOFF COMPONENTS

W.J. Schreur
March 2019

Title Impacts of climate change on flow composition using a model tailored to runoff components

Author Wouter Jan Schreur

Institute University of Twente
Institute of Geophysics, Polish Academy of Sciences

Supervisors Dr. ir. M.J. Booij
University of Twente, Department of Water Engineering and Management

Dr. M.S. Krol
University of Twente, Department of Water Engineering and Management

Advisor Prof. dr. hab. eng. R.J. Romanowicz
Institute of Geophysics, Polish Academy of Sciences; Department of Hydrology and Hydrodynamics

Date 12 March 2019

Summary

Over the past decades various studies have indicated that climate change and its accompanying hydrological impacts are a prevalent issue. Without proper measures the impact of floods and droughts can extend to various water dependent sectors including agriculture, forestry, fishing, hydropower and tourism. Generally, climate change impact on river discharge is assessed based on projected changes to the total runoff. It is however argued that looking exclusively at the total river discharge is not a sufficient indicator and additional insights in the runoff would be a step towards improvements on runoff modelling and gaining insight in climate change impacts. The goal of this research is to gain insight in the runoff components that together make up the total runoff and how to calibrate a hydrological model such that the skill at which the individual runoff components are simulated improves. These new insights will then be applied to calibrate a hydrological model tailored towards simulating runoff components and assess the impacts of climate change not only on the total runoff but also the impact it has on the runoff components and the composition of the total runoff.

For this research, hydrological modelling will be done using the Hydrologiska Byråns Vattenbalansavdelning (HBV) model. Three Polish catchments: Biala Tarnowska, Dunajec and Narewka catchments are used as test cases in this research.

To find if there is a relationship between the criteria that are used in model calibration and the skill at which the HBV model simulates the runoff components two objective functions have been used for model calibration. The two criteria or objective functions that are used for model calibration are the Nash-Sutcliffe efficiency criterion (NS) that emphasised high flows and the logarithmically transformed Nash-Sutcliffe (NSL) which emphasises baseflow. The two objective functions are used in a weighted manner by assigning a weight to each function to be able to later identify a trade-off between the objective functions. The weights assigned to both objective functions are varied between 0% to 100% at increments of 10% while keeping the sum of the weights equal to 100%. Calibration was done using the SCEM-UA calibration algorithm which resulted in 11 unique parameter sets for each catchment, each corresponding to a combination of NS and NSL function weights.

The contributions of the runoff components are derived from the total runoff using the Wittenberg baseflow filter (Wittenberg, 1999). The skill at which the runoff components are simulated is assessed by using the NS as performance indicator and comparing the individual runoff components derived from simulations to those derived from the observations. Correlation between the skill at which runoff components are simulated and the NSL weight used in model calibration indicates that, for all three catchments, there is a significant correlation between the NSL weight and the HBV model its ability to skilfully simulate the baseflow component. A significant correlation between the NSL weight used in calibration and the skill at which the HBV model simulates the fast runoff component was only found for the Narewka catchment. Because the goal is to improve on the skill at which runoff components are simulated, the final calibration has been done using exclusively the NSL as performance indicator for model calibration.

Using the HBV model that is calibrated for the three catchments using the NSL as performance indicator, climate change impacts on the total runoff have been assessed and additionally the impact that climate change has on the runoff components and the composition of the runoff are assessed. For climate change (re)assessment synthetic climate data is used from the EURO-CORDEX initiative. The datasets consist of precipitation and temperature simulations generated by seven combinations of General Circulation Models (GCM) and Regional Climate Models (RCM)

Assessment of climate change impacts on projected flow resulted in findings that correspond to earlier modelling studies that have used the considered catchments as case studies (Osuch et al., 2016; Piniewski, 2017). The annual total runoff is projected to increase with the largest projected increase observed in the winter (December, January and February) and spring (March, April and May) periods.

Separation of the runoff in the fast runoff component and the baseflow component indicated that there are differences in the composition of the total runoff between the three catchments for the observational period. When projected flows are assessed differences between the catchment are still present but differences between the simulations that are done using the GCM/RCM combinations are also present. These differences between the seven GCM/RCM combinations appeared to be consistent between the catchments and are assumed to be related to the individual GCM and/or RCM models that are used in simulating the climate data. Looking at the impact that projected climate change will have on the composition of the runoff indicated that the composition of the total runoff is not projected to change in the future for either of the climate models.

Previously, climate change projections have shown that the intensity of precipitation events is projected to increase which results in the expectations that more fast runoff will occur. Findings from this research however do not support this expectation. This might be caused by not taking into account changes that the catchments themselves may undergo over the upcoming decades. Wang & Cai (2010) have shown that the main driving force in changes in the flow composition is human interference (e.g. urbanisation or canalisation), an aspect that is not taken into account in this study. Another explanation for the absence of these changes can be found in the climate data that has been used in this research. Simulations from the GCM or downscaling to a RCM could have resulted in climate data that does not contain this increase in intensity but rather display a gradual uptrend in the precipitation. These possible causes however were outside of the scope of this research and have not been further pursued.

In conclusion, there appears to be a significant relationship between objective functions that are used in model calibration and the skill at which runoff components can be simulated. This again shows the importance of selecting the most suited objective functions according to the research objective. But even while new insights have been gained in this area it displays that the impacts of climate change on river runoff might be restricted to changes in the total runoff after all. And that the composition of the runoff is not projected to change when compared to runoff simulations of the present situation. To conclude this research, several recommendations have been made that might be a worthwhile endeavour to pursue in order to be able to make these results more applicable wider variety of cases and to further improve on modelling runoff components.

Table of Contents

1	Introduction	5
1.1	Background and Relevance	5
1.2	Problem Description	6
1.3	Research objective	6
1.4	Research Strategy and Reading Guide	7
2	Study area and data sets.....	9
2.1	Catchments	9
2.1.1	Biała Tarnowska	10
2.1.2	Dunajec	10
2.1.3	Narewka	10
2.2	Observational data sets.....	11
2.2.1	Discharge	11
2.2.2	Precipitation.....	12
2.2.3	Temperature	13
2.3	Climate change data sets	14
3	Methodology.....	17
3.1	Hydrological model	17
3.1.1	Model choice	17
3.1.2	Model description and model equations.....	18
3.2	Sensitivity analysis.....	21
3.2.1	Objective functions	21
3.2.2	Sobol's method	22
3.3	Model calibration	24
3.3.1	Calibration algorithm choice.....	24
3.3.2	Calibration algorithm	24
3.3.3	Calibration and validation period	25
3.4	Simulation of runoff components	25
3.4.1	Hydrograph separation	25
3.4.2	Simulation of runoff components.....	26
3.5	Climate change impact.....	27
4	Results.....	29
4.1	Sensitivity Analysis	29

4.2	Model calibration	31
4.2.1	Parameter ranges	31
4.2.2	Calibration Results	33
4.3	Simulation of runoff components	36
4.4	Trade-off between objective functions.....	37
4.5	Climate change impact.....	38
4.5.1	Model performance on reference period.....	38
4.5.2	Climate change impact on the total runoff.....	40
4.5.3	Climate change impact on the runoff components	41
4.5.4	Projected changes in low flows	44
5	Discussion	47
5.1	Datasets	47
5.2	Model calibration	47
5.3	Results	48
6	Conclusion.....	51
7	Recommendations	52
8	References	53
9	Appendices.....	59
A.	Appendix A	59
B.	Appendix B.....	62
C.	Appendix C.....	63
D.	Appendix D	66

List of Figures

Figure 2-1: Geographical locations of the considered catchments. (Romanowicz et al., 2016).....	9
Figure 2-2: Daily mean discharges for the Biała Tarnowska, Dunajec and Narewka catchments for the 1971-2010 period	11
Figure 2-3: Mean monthly precipitation values for the observation period 1971-2010.....	12
Figure 2-4: Observed mean daily temperature for the 1971-2010 period.....	13
Figure 2-5: Annual sum precipitation for the Biała Tarnowska, Dunajec and Narewka catchments for the 1971-2100 period from the seven GCM/RCM combinations	14
Figure 2-6: Annual mean temperature for the Biała Tarnowska, Dunajec and Narewka catchments for the 1971-2100 period from the seven GCM/RCM combinations	15
Figure 3-1: HBV model structure, adopted from Knoben (2013)	18
Figure 3-2: Visual representation of the temperature interval and temperature threshold (Knoben, 2013).....	19
Figure 3-3: Wittenberg's baseflow separation applied to the Biała TArnowska catchment for the year 1976.....	26
Figure 4-1: Results of variance decomposition for the Biała Tarnowska catchment	30
Figure 4-2: Results of variance decomposition for the Dunajec catchment.....	30
Figure 4-3: Results of variance decomposition for the Narewka catchment	30
Figure 4-4: Calibration results for the Biała Tarnowska catchment	33
Figure 4-5: Calibration results for the Dunajec catchment.....	34
Figure 4-6: : Calibration results for the Narewka catchment	35
Figure 4-7: NS Scores for the fast runoff and baseflow components for the Biała Tarnowska catchment.....	36
Figure 4-8: NS scores for the fast runoff and baseflow components for the Dunajec catchment	36
Figure 4-9: NS scores for the fast runoff and baseflow components for the Narewka catchment.....	37
Figure 4-10: Modelled Annual mean flow from the Biała Tarnowska, Dunajec and Narewka catchments for the 1971-2100 period	41

List of Tables

Table 2-1: Observed mean flow and standard deviation for the years 1971-2010.....	12
Table 2-2: Minimum, mean and maximum observed yearly precipitation for the Biała Tarnowska, Dunajec and Narewka catchments.....	13
Table 2-3: List of GCM/RCM combinations used in this study	14
Table 3-1: SCEM-UA algorithm parameters (Vrugt et al., 2003b)	25
Table 4-1: HBV model parameters that will be taken into account for model calibration per catchment	31
Table 4-2: Definitive parameter ranges used in calibration of the HBV model for the Biała Tarnowska catchment ..	31
Table 4-3: Definitive parameter ranges used in calibration of the HBV model for the Dunajec catchment	32
Table 4-4: Definitive parameter ranges used in calibration of the HBV model for the Narewka catchment.....	32
Table 4-5: Default parameter values for the HBV model (SMHI, 2006)	32
Table 4-6: Correlations between the NS scores of the components and the weight assigned to the NSL	37
Table 4-7: Mean runoff from the Biała Tarnowska catchment per GCM/RCM combination and deviation from the observed mean runoff.....	39
Table 4-8: Mean runoff from the Dunajec catchment per GCM/RCM combinations and deviation from the observed mean runoff.....	39
Table 4-9: Mean runoff from the Narewka catchment per GCM/RCM combinations and deviation from the observed mean runoff.....	39
Table 4-10: changes in percentage per year in modelled annual runoff over the 1971-2100 period for the Biała Tarnowska, Dunajec and Narewka catchments.....	41
Table 4-11: Derived BFI for the Biała Tarnowska catchment from runoff simulations for each of the seven GCM/RCM combinations for the reference, near-future and far-future period	42
Table 4-12: Derived BFI for the Dunajec catchment from runoff simulations for each of the seven GCM/RCM combinations for the reference, near-future and far-future period	42
Table 4-13: Derived BFI for the Narewka catchment from runoff simulations for each of the seven GCM/RCM combinations for the reference, near-future and far-future period	42
Table 4-14: Seasonal BFI contributions to the total flow for the Biała Tarnowska catchment for the reference, near-future and far-future periods	43
Table 4-15: Seasonal BFI contributions to the total flow for the Dunajec catchment for the reference, near-future and far-future periods	43
Table 4-16: Seasonal BFI contributions to the total flow for the Narewka catchment for the reference, near-future and far-future periods	43
Table 4-17: Q90 for the Biała Tarnowska, Dunajec and Narewka catchments derived from the observed runoff for the reference period.....	44
Table 4-18: Mean Q90 for the Biała Tarnowska, Dunajec and Narewka catchments derived from the simulated runoff for the reference, near-future and far-future period	44

1 INTRODUCTION

This chapter of the report will be used to introduce the topic of this research and will set the scope of what this research will consist of. In section 1.1 background information on the topic will be discussed and the relevance of this research will be pointed out. The problem description is presented in section 1.2 along with the research questions that have been defined in section 1.3. An overview of how the report will be structured is presented in section 1.4.

1.1 BACKGROUND AND RELEVANCE

From studies and observations it has become more and more apparent that climate change and its hydrological impacts are a prevalent issue. Without proper measures the impact of floods and droughts extend to various water dependent sectors, including agriculture, forestry, fishing, hydropower and tourism. (Demirel et al., 2013) Additionally extreme events can have direct societal impacts by disrupting e.g. domestic water supply and infrastructure. Therefore, it is important to gain more insight in the occurrence of hydrologically extreme events and projected changes in their magnitude and probability of occurrence (CHIHE, 2016). In the Intergovernmental Panel on Climate Change's Assessment Report 5 it is described that, over mid-latitude regions, it is very likely that extreme precipitation events will become more frequent and also become more intense (Pachauri & Meyer, 2014) which leads to an increased risk of urban- and flash flooding caused by rainfall. In addition to this, projections also show a shorter snow season in mountainous areas which means that less snow will accumulate which leads to a decreased risk of spring floods (WHO, JRC, & EEA, 2008).

Translation of climatic variables and catchment characteristics to river discharge is done using hydrological models. Many studies have been done into the functioning of these models as well as the application of the models on case studies. In the majority of the case studies where hydrological models are applied to model runoff from catchments the focus has been on the total runoff (e.g. Lindström et al., 1997; Beven, 2012). Also, for assessment of the impacts of climate change the effects are generally assessed based on changes to the projected total runoff (e.g. Bisterbosch, 2010; Osuch et al., 2016). For various Polish catchments for example, studies on climate change impact have shown that projected changes will lead to a shift in the timing of runoff and change in the magnitude of runoff peaks. The flood season is expected to shift from March-April to January-February due to the earlier snowmelt (Romanowicz et al., 2016).

The total runoff can also be seen as the combined sum of the runoff components, a faster, direct runoff component and, a slower, baseflow component. These individual components often go unobserved as generally only the total runoff is measured and the origins of the runoff remain unknown. Retracing the origin of the baseflow can be done by tracer analysis if the data is present in addition to the observations of the runoff. Alternatively, the baseflow can be derived from the total runoff by making use of filtering techniques. These filtering techniques can be based on different measurable aspects of the hydrograph but are most commonly based on the recession parameter that is derived from the receding part of the hydrograph. Studies into the impact of climate change on the total runoff are common and widespread but studies into runoff components and the composition of the total runoff are far more uncommon.

For proper functioning of a hydrological model it is paramount that the correct parameter values are found for the hydrological model by calibrating them. In model calibration one or more objective functions can be used to assess the model performance by comparing the model output to observations. Different objective functions emphasize different parts of the hydrograph during the model calibration and the correct objective function should be determined a-priori according to the goal of the research (Chang, 2014). Often a single objective function is used in

model calibration (e.g. Knoben, 2013; Osuch et al., 2016; Romanowicz et al., 2016) but there are also various reported cases where a combination of objective functions was used in model calibration (e.g. Dawdy et al., 1971; Li et al., 2014; Lv et al., 2018). Model calibration using multiple objective functions in e.g. the aforementioned studies was done by assigning static weights to the objective functions which were arbitrarily assigned. Because of the static weights that were assigned to the different objective functions it is uncertain if the weighting of the functions has resulted in the best parameterisation of the model of the research purpose.

1.2 PROBLEM DESCRIPTION

Assessing impacts of climate change by looking at the total river discharge does not give full insight in the alterations the river discharge might undergo. Even looking at more specific parts of the hydrograph, e.g. the maximum, mean or seasonal flows does not show the full picture of the hydrological impact of climate change on river runoff. A more thorough way to assess the changes a river system undergoes is to decompose the runoff into its components that together make up the total runoff and look at the impact that climate change has on the individual components and the composition of the total runoff.

Because the individual components of the runoff are usually not observed (Romanowicz, 2017), calibration and validation of hydrological models is therefore done based on the hydrograph representing the total runoff. This might lead to a model calibration that performs best for simulating the total runoff but might not correctly describe the individual runoff components. The underlying problem herein is that little research has been done into a calibration method that can be applied such that the model output not only corresponds to the observed total runoff but that also the derived runoff components are simulated correctly. It is known that different objective functions emphasize different parts of the hydrograph and objective functions can be chosen according to the goal of the research. However, the impact that different objective functions have on the model its ability to simulate the individual runoff components is a topic in which little research has been done. This limitation leads to the uncertainty on the reliability of more detailed analysis on the effect of changing climatological conditions not only on the projected total runoff but also on the runoff components and the composition of the runoff.

1.3 RESEARCH OBJECTIVE

The goal of this research is to find whether there is a relationship between the objective functions that are used during model calibration and the ability of a hydrological model to correctly simulate runoff components in addition to correctly simulating the total runoff. This potential relationship will then be used to calibrate a hydrological model that is tailored towards simulation of runoff components. With this calibrated model, the impact of climate change will be assessed for a test case considering three Polish catchments. The impact of climate change will be evaluated by assessing the impact that projected climate change has on the composition of the runoff in addition to the impact it has on the total runoff.

To reach these objectives and guide the research the following research questions have been formulated:

1. What is the trade-off between objective functions for model calibration for the accuracy at which runoff components are simulated?
2. Which parameter set allows the HBV model to correctly simulate both the total runoff and the runoff components for the Biała Tarnowska, Dunajec and Narewka catchments?
3. What are the contributions of the runoff components to the observed runoff for the Biała Tarnowska, Dunajec and Narewka catchments?
4. What are the impacts of projected climate change on the runoff components and the composition of the runoff?

1.4 RESEARCH STRATEGY AND READING GUIDE

To answer the aforementioned research questions and achieve the objective of this research the research and report are structured as follows. Firstly, the HBV model will be set up with a reduced number of parameters. The parameters which will be involved in the model calibration are determined per catchment by executing a sensitivity analysis. The model will be calibrated for various combinations of weights assigned to the Nash-Sutcliffe and the logarithmic Nash-Sutcliffe objective functions. Multiple calibrations for various objective function weights allow for a comparison between the scores achieved on the objective functions and the weights assigned to the objective functions. From this comparison insight will be gained in the trade-off between the objective functions and the model its ability to correctly simulate the runoff components. Based on the trade-off between the objective functions the most appropriate weights that will be assigned to the individual objective functions will be determined in order to allow for the most accurate simulation of the individual runoff components.

With the model being correctly set up and calibrated the impact of climate change can be assessed. The impacts of climate change will firstly be evaluated on the total runoff before going into a more detailed analysis of the impact that climate change is projected to have on the runoff components. Assessing the impact of climate change will be done by comparing the projected changes for the near-future (2021-2050) and far-future (2071-2100) to the reference period (1976-2005).

Climate change impact on the runoff components will be evaluated by looking more closely at the composition of the total runoff. The total runoff will be separated into the baseflow components and the quick runoff component. The contribution of the two individual components to the runoff will be used to indicate whether climate change will impact the composition of projected flows for the near-future and far-future relative to the composition of the flow in the reference period.

The Biała Tarnowska, Dunajec and Narewka catchments that are considered in this research as well as the datasets what will be used will be presented in chapter 2. In chapter 3, the aforementioned approach to the research will be discussed in more detail. The results that are obtained will be presented in chapter 4 and discussed in chapter 5 with the final conclusions and recommendations being presented in chapters 6 and 7.

2 STUDY AREA AND DATA SETS

In this chapter of the report the data sets that will be used in this study will be presented. In chapter 2.1 the catchments that will be used in the case study are presented along with a description of the characteristics of the catchments. Chapter 2.2 will be used to describe the datasets containing the observational data and in chapter 2.3 the datasets containing the climate projections will be presented.

2.1 CATCHMENTS

In the case study that will be executed in this research three Polish catchments will be considered. The three catchments that are chosen for this purpose are the Biała Tarnowska, the Dunajec and the Narewka catchments. In the following sections these catchments will be individually described and characterized.

The choice for these specific catchments has been made based on previous research. The Polish-Norwegian project Climate Change Impact on Hydrological Extremes (CHIHE) has identified catchments that were suited for rainfall runoff and climate change modelling. Romanowicz et al. (2016) describes the selection procedure that was used to identify these catchments. In this study, ten nearly-natural Polish catchments were identified and flood regimes have been attributed to each catchment.

In earlier modelling studies from the CHIHE project for these catchments, rainfall runoff modelling has been done by using the HBV model. The accuracy at which their calibrated models were able to reproduce the observed river runoff has been used as criteria for catchment selection in this study. Both the calibration and validation periods are taken into account in this consideration. This choice should ensure that catchments with the best data quality will be used. In Figure 2-1 a map is displayed where the geographical location of the catchments can be found along with the flood regime attributed to each catchment.

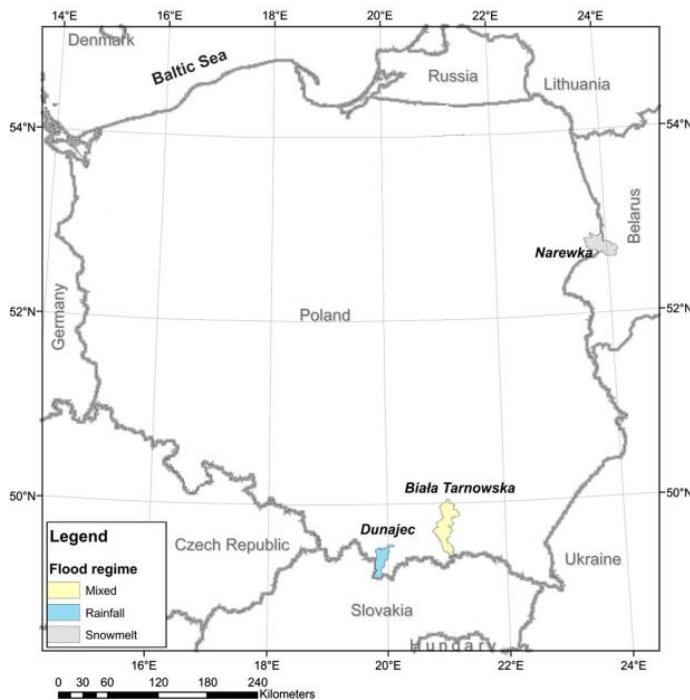


FIGURE 2-1: GEOGRAPHICAL LOCATIONS OF THE CONSIDERED CATCHMENTS. (ROMANOWICZ ET AL., 2016)

2.1.1 BIAŁA TARNOWSKA

The Biała Tarnowska catchment is located in the southern regions of Poland in the Carpathian Mountains and extends north from the Polish-Slovakian border. The source of the river has an elevation of 730 m above mean sea level and the total length of the Biała Tarnowska is 101.8 km along which the river banks are unregulated and in a natural state. The catchment area of the Biała Tarnowska that is drained by the river is 956.9 km² and is in a nearly-natural state (Napiorkowski et al., 2014).

The southern, mountainous, region of the catchment representing about 25% of the catchment area is covered with woodland and has relatively steep river slopes which are in the range of 10‰. The northern regions of the catchment can be described as deep river valleys where fields, meadows and pastures predominate. In this area of the catchment the river slope is much gentler in the range of 0.9 – 5 ‰. Biała Tarnowska is a perennial river that is characterized by its mixed runoff regime that contains elements of both snowmelt and rainfall as driving mechanisms for runoff generation (Romanowicz et al., 2016). T

2.1.2 DUNAJEC

The Dunajec catchment is situated in southern Poland in the Tarta Mountains and is formed at the confluence of the Czarny Dunajec (Black Dunajec) and the Biały Dunajec (White Dunajec). The Dunajec River has a length of 274 km of which 27 km forms a natural border between Slovakia and Poland.

The drainage area of the Dunajec basin that discharges to the Dunajec River is 681.1 km² of which nearly 60% is used for agricultural purposes. The Dunajec is a nearly natural the river with unregulated banks that are in a natural state and an average slope of the Dunajec is 8‰ (Rowinsky, 2013; Kundewicz et al., 2016). Romanowicz et al. (2016) classified the runoff regime of the Dunajec River as a predominantly rainfall fed river.

2.1.3 NAREWKA

The Narewka Catchment is located in the north-eastern regions of Poland on the Polish Plain and extends over the border with Belarus. The area of the catchment is 635.3 km² of which the largest part is on Polish territory. The Narewka river that is fed from this catchment has a length of 61.1 km of which approximately 22 km in Belarus with the slope of the river ranging between 0.35‰ and 0.64‰ (Jedrzejska & Jedrzejski, 1998).

In Romanowicz et al. (2016) the Narewka catchment was classified as a nearly-natural catchment with a flood regime that is predominantly fed by snowmelt. Nearly the entire catchment (88%) is covered with forests. Of the remaining area 11% is used for agriculture.

2.2 OBSERVATIONAL DATA SETS

The observational datasets that are used for this study contain observations on the river discharge and climatological variables for the selected catchments. The datasets contain observations covering the period from 1971 until the 2010 measured at daily intervals. The datasets have been checked on data quality i.e. the datasets contain no obvious outliers and/or missing values. In the following sections the available datasets will individually be described briefly and presented in figures.

2.2.1 DISCHARGE

Discharge data as provided by the Institute of Geophysics Poland (IGF PAN) is the observed river discharge at the gauging station at the outlet of the catchment. The river discharge is determined based on water level measurements which have been converted using rating curves. In Figure 2-2 the mean daily observed discharge for each of the three catchments are presented. Peaks in the discharge can be observed mainly in the spring and summer periods. These spring floods are largely the result of snowmelt whereas discharge peaks in the summer are caused by precipitation events. Mean flow and standard deviation for the catchments are presented in Table 2-1 **Error! Reference source not found..**

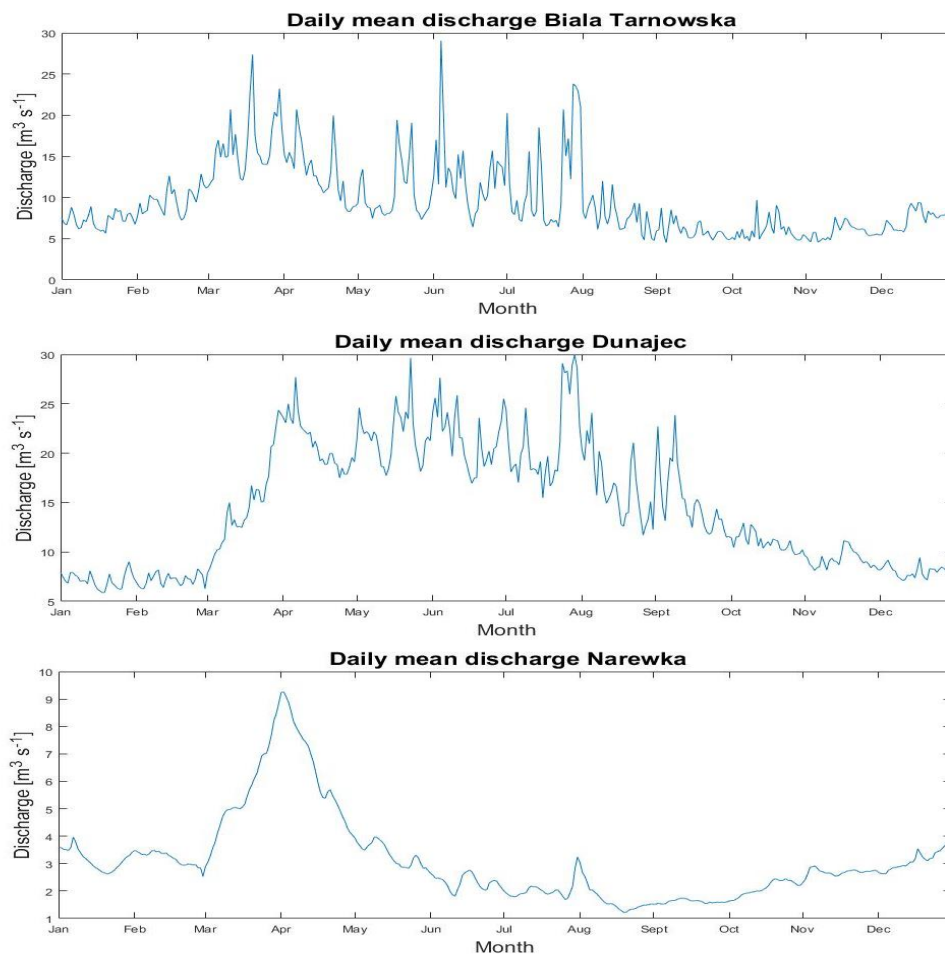


FIGURE 2-2: DAILY MEAN DISCHARGES FOR THE BIAŁA TARNOWSKA, DUNAJEC AND NAREWKA CATCHMENTS FOR THE 1971-2010 PERIOD

TABLE 2-1: OBSERVED MEAN FLOW AND STANDARD DEVIATION FOR THE YEARS 1971-2010

Catchment	Mean flow [$\text{m}^3 \text{s}^{-1}$]	Standard deviation [$\text{m}^3 \text{s}^{-1}$]
Biała Tarnowska	9.5	20.3
Dunajec	14.6	17.1
Narewka	3.1	3.5

2.2.2 PRECIPITATION

Precipitation data for the catchments is taken from one or a combination of multiple meteorological observation stations located in or close to the catchment. The Narewka catchment is the only catchment that makes use of observations from only one measurement station. The data sets of the Biała Tarnowska and Dunajec make use of data derived from 5 and 3 measurement stations respectively. The areal average precipitations that is used in this study is derived from the observations from the individual meteorological stations and averaged to one representative value for the entire catchment by using Thiessen polygons (Benninga et al., 2017). Precipitation values are provided in mm at daily measurement intervals.

In Figure 2-3 the average monthly precipitation over the observation period is presented to show how the precipitation is distributed over the year. It can be seen that the Biała Tarnowska and Dunajec catchments where the flood regime is dominated by rainfall or is a mixed regime the summer precipitation is relatively much higher than in the snowmelt dominated Narewka catchment. Annual minimum, mean and maximum observed values for the precipitation over the 1971-2010 period are presented in Table 2-2.

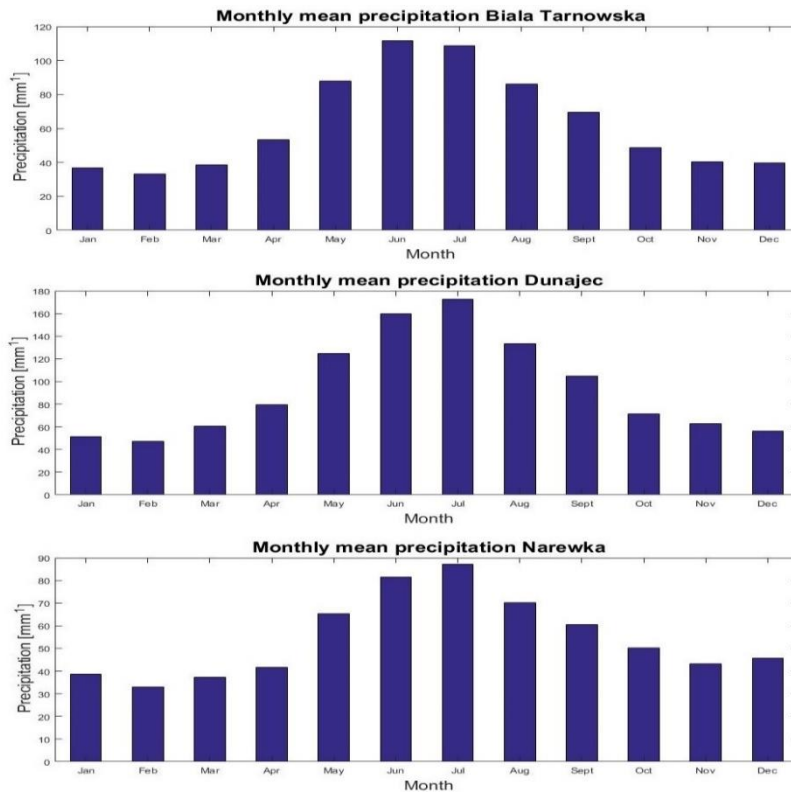


FIGURE 2-3: MEAN MONTHLY PRECIPITATION VALUES FOR THE OBSERVATION PERIOD 1971-2010

TABLE 2-2: MINIMUM, MEAN AND MAXIMUM OBSERVED YEARLY PRECIPITATION FOR THE BIAŁA TARNOWSKA, DUNAJEC AND NAREWKA CATCHMENTS

Catchment	Minimum observed precipitation [mm]	Average observed precipitation [mm]	Maximum observed precipitation [mm]
Biała Tarnowska	552	752	1 073
Dunajec	816	1 120	1 460
Narewka	448	651.1	933

2.2.3 TEMPERATURE

From the same measurement stations that are used for the precipitation observations the temperature observations are obtained for the three catchments. In Figure 2-4 the mean daily observed temperature for the 1971-2010 period is displayed in degrees Celsius. The temperature observations are used in calculating the potential evapotranspiration according to the method of Hamon (Hamon, 1961) and as model inputs for the snow accumulation and snowmelt routines of the hydrological model.

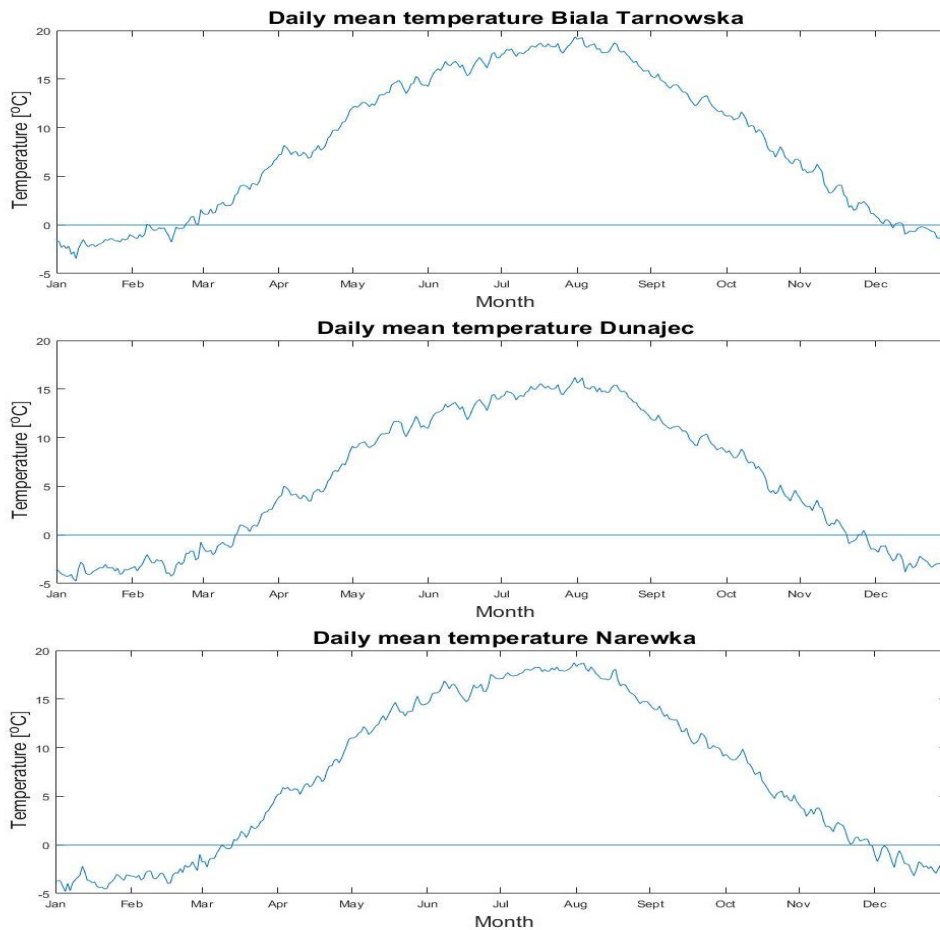


FIGURE 2-4: OBSERVED MEAN DAILY TEMPERATURE FOR THE 1971-2010 PERIOD

2.3 CLIMATE CHANGE DATA SETS

The datasets containing the future climate projections contain the results from several climate model simulations. The climate projection data used in this research consists of the daily temperature and precipitation and were obtained from the EURO-CORDEX initiative (<http://www.euro-cordex.net/>). The climate change scenario that these projections represent is the RCP 4.5 scenario which is described in the Fifth Assessment Report (AR5) by the Intergovernmental Panel on Climate Change (IPCC, 2013).

All climate simulations are done using a General Circulation Model (GCM) and a Regional Climate Model (RCM). In total seven GCM/RCM combinations are used to generate the dataset resulting in an ensemble of seven different projections. The seven GCM/RCM combinations that are used to generate the climate change projections are presented in Table 2-3 along with the affiliated institute (Meresa & Romanowicz, 2017).

TABLE 2-3: LIST OF GCM/RCM COMBINATIONS USED IN THIS STUDY

	GCM	RCM	Institute
1	EC-EARTH	RCA-4	Swedish Meteorological and Hydrological Institute
2	EC-EARTH	HIRHAM5	Danish Meteorological Institute
3	EC-EARTH	CCLM-4-8-17	NCAR UCAR
4	EC-EARTH	RACMO22E	Danish Meteorological Institute
5	MPI-ESM-LR	CCLM-4-8-17	Max Planck Institute for Meteorology
6	MPI-ESM-LR	RCA4	Max Planck Institute for Meteorology
7	CNRM-CM5	CCLM4-8-17	CARFACS, France

In Figure 2-5 the projected annual precipitation from the seven GCM/RCM models is presented for the 1971-2100 period for the three catchments considered in this study. Each coloured dot represents a GCM/RCM combination and the black line represents the ensemble mean annual precipitation of the seven GCM/RCM combinations. All three catchments show an upward trend in the mean annual precipitation with the strongest upward trend for the Narewka catchment.

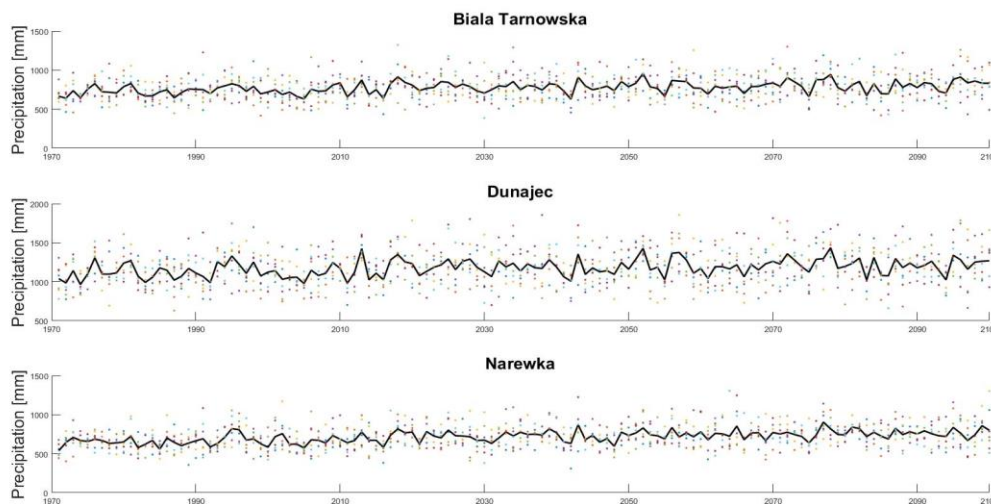


FIGURE 2-5: ANNUAL SUM PRECIPITATION FOR THE BIAŁA TARNOWSKA, DUNAJEC AND NAREWKA CATCHMENTS FOR THE 1971-2100 PERIOD FROM THE SEVEN GCM/RCM COMBINATIONS

In Figure 2-6 the projected annual mean air temperatures are presented for the Biała Tarnowska, Dunajec and Narewka catchments for the 1971-2100 period obtained from the seven GCM/RCM combinations. Each coloured dot represents a GCM/RCM combination and the black line represents the ensemble mean annual air temperature between the seven GCM/RCM combinations. Also, for the temperature projections, for all three catchments an upward trend is observed. The largest projected increase in annual mean temperature is observed for the Dunajec catchment.

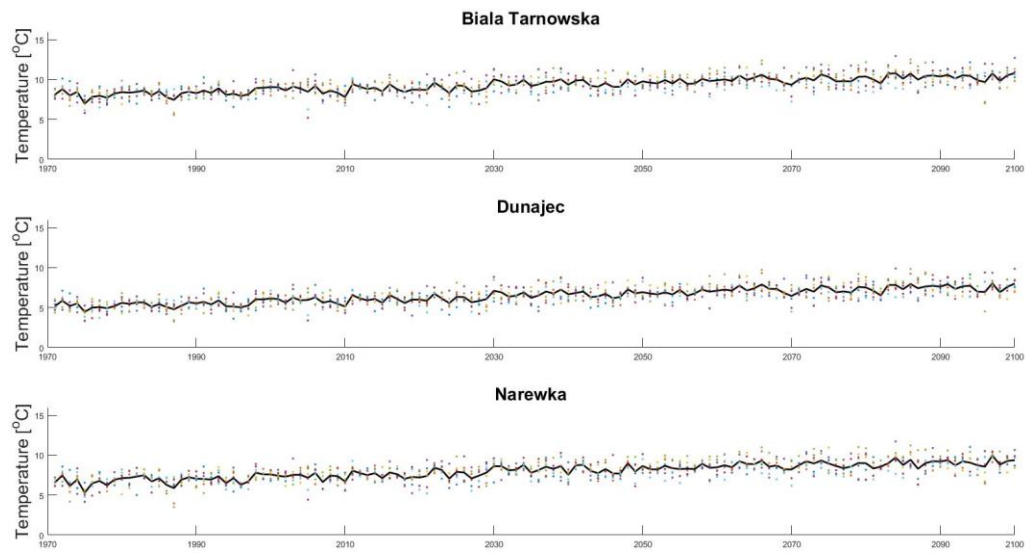


FIGURE 2-6: ANNUAL MEAN TEMPERATURE FOR THE BIAŁA TARNOWSKA, DUNAJEC AND NAREWKA CATCHMENTS FOR THE 1971-2100 PERIOD FROM THE SEVEN GCM/RCM COMBINATIONS

3 METHODOLOGY

In this chapter the approach that will be taken to the research and answering the research questions will be presented. Section 3.1 will elaborate on the choice of which hydrological model will be used and describe how the hydrological model functions. The sensitivity analysis that will be applied is presented in section 3.2. The approach to model calibration will be presented in section 3.3 including considerations made on what calibration algorithm will be applied and which objective functions will be used. Section 3.4 will go into how the runoff components will be derived from the model outputs and the methods that will be used to assess how well the individual runoff components are simulated. Lastly in section 3.5 the approach to assessing climate change impacts on both the total runoff and the individual runoff components will be presented.

3.1 HYDROLOGICAL MODEL

This chapter will elaborate on the choice for using the Hydrologiska Byråns Vattenbalansavdelning (HBV) model in section 3.1.1. The model structure, model equations and model parameters will be presented in section 3.1.2.

3.1.1 MODEL CHOICE

Models are a simplified representation of real-world systems (Stevenson, 2002). For hydrological models this means that the dominant processes that govern the conversion from precipitation to runoff are simplified to a set of equations. Using precipitation, temperature and potential evapotranspiration as model inputs, hydrological models enable the modeler to obtain an estimate of the runoff that is generated from the catchment. This has made hydrological models an essential component in many fields, including spatial planning, water quality modelling and flood and drought forecasting. Besides these applications, hydrological models are also an important tool for assessing the impacts of climate change on river discharge.

A large number of hydrological models exist, all using different model structures and/or representations of the physical processes that lead to the generation of runoff (Singh, 1995). Hydrological models can be classified into various archetypes, e.g. conceptual models, physics-based models or empirical models (Pechlivanidis et al., 2011). In this research the conceptual Hydrologiska Byråns Vattenbalansavdelning (HBV) model will be applied. Conceptual models represent the hydrological processes that are considered to be dominant in the translation from climatological input variables to runoff following a predetermined model structure. Not all model parameters have a direct physical interpretation and therefore have to be estimated by calibrating them against observed data (Pechlivanidis et al., 2011; Jajarmizadeh et al., 2012).

The HBV model was originally developed by the Swedish Meteorological and Hydrological Institute and has a long history with its first application as early as 1973 (Bergström and Forsman, 1973). Ever since its development and first applications the model has been improved and modified which has also led to a steady increase of the scope of the model and its applications (Lindström et al., 1997). Since its initial development the HBV model has been successfully applied in over 90 countries for various applications including forecasting (e.g. Bergström & Lindström, 2015; Benninga et al., 2017) and climate change impact studies (e.g. Booij, 2004; Romanowicz et al. 2016; Kundzewicz et al., 2017). These aforementioned studies have shown that the HBV model is able to skilfully model rainfall runoff in terms of total flow.

Besides the widespread successful application of the HBV model another argument for the HBV model is that the model outputs are dependent on the climatological inputs: temperature, potential evapotranspiration and precipitation of which historical data as well as future projections are available. This makes the HBV model a suitable

model for assessing climate change impacts as seen from many previous studies (e.g. Tian et al., 2013; Al-Safi & Sarukkalige, 2017; Worqlul, 2018).

3.1.2 MODEL DESCRIPTION AND MODEL EQUATIONS

In Figure 3-1 the model structure of the HBV-96 model is displayed. The model consists of five storages that are linked together by the fluxes between them. Inputs for the model are the temperature (T) in [°C], potential evapotranspiration (PET) in [mm d⁻¹] and the precipitation (P) in [mm d⁻¹]. The precipitation is also the flux going into the model. Outgoing fluxes are the evapotranspiration (ET) in [mm d⁻¹] and the runoff (Q) in [mm d⁻¹]. The total runoff that is calculated by the model consists of a fast component and a slow component. The fast component is generated from a nonlinear reservoir whereas the slow component is generated from a linear storage box (Bergström, 1992).

In the HBV-96 model four routines can be identified: (1) precipitation, (2) soil moisture, (3) fast response and (4) slow response. Each routine is governed by its own model parameters with a total of 14 parameters in the HBV-96 model that can be calibrated.

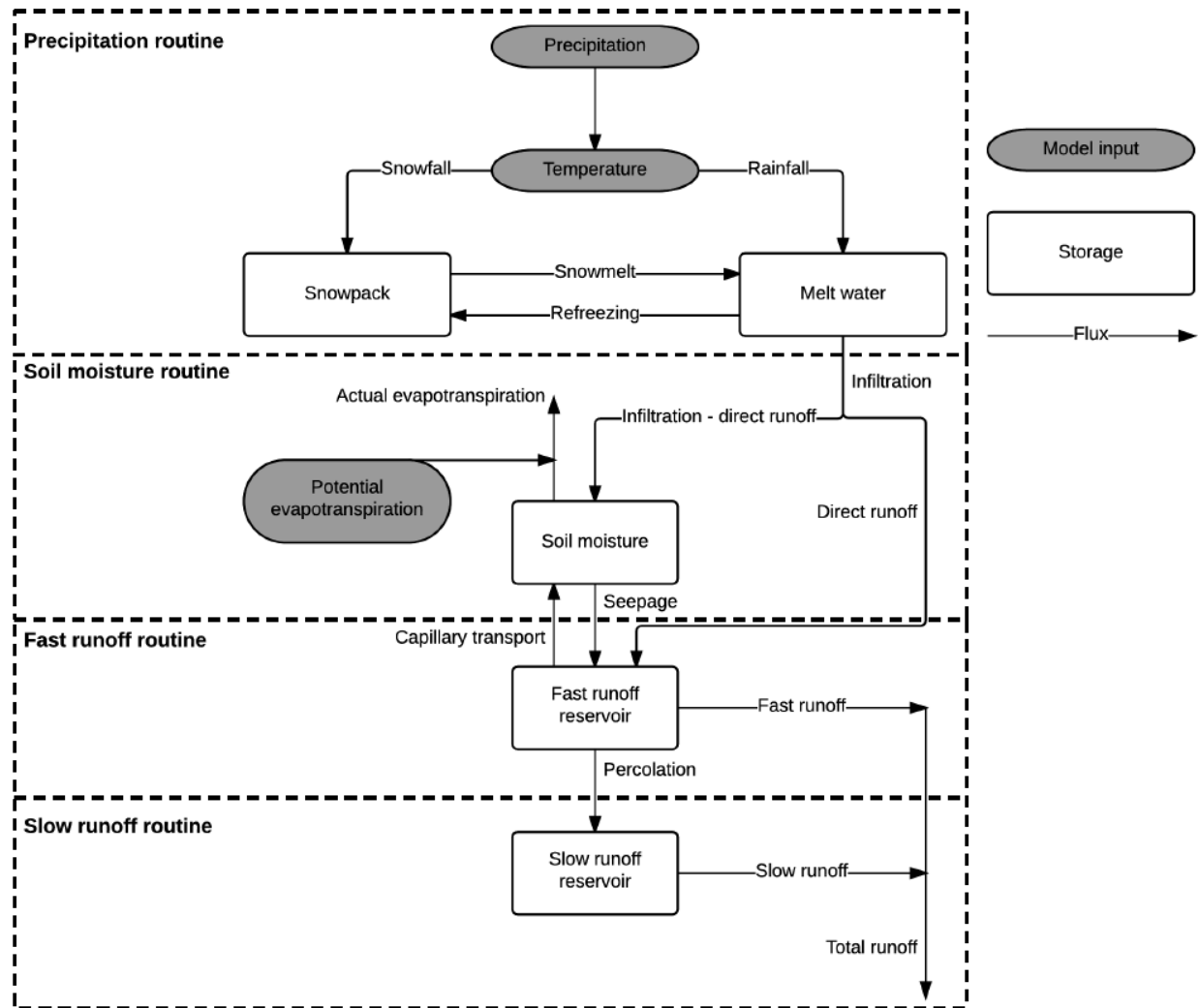


FIGURE 3-1: HBV MODEL STRUCTURE, ADOPTED FROM KNOBEN (2013)

Precipitation routine

In the precipitation routine the total precipitation is split up into rainfall and snowfall or a combination of the two. At every time step (t) the total precipitation P is divided into rainfall P_r and snowfall P_s based on the air temperature T . Parameters TT in $^{\circ}\text{C}$ and TTI $^{\circ}\text{C}$ are used to define an interval of size TTI centred around TT along which it is assumed that precipitation will be a mix between rain and snow, linearly decreasing from 100% snow at the lower threshold to 0% snow at the upper threshold. Figure 3-2, adopted from Knoben (2013), gives a visual representation of the TT and TTI parameters and the interval and threshold that they define.

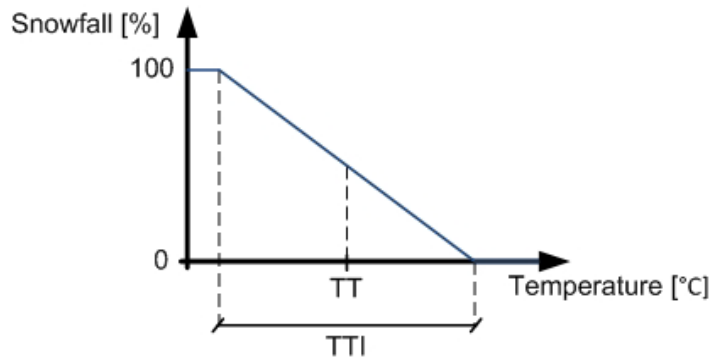


FIGURE 3-2: VISUAL REPRESENTATION OF THE TEMPERATURE INTERVAL AND TEMPERATURE THRESHOLD (KNOBEN, 2013)

This distinction between snow and rain allows to direct them to different storage boxes; the snowpack (S_{sp}) in [mm] and the melt water storage (S_{mw}) in [mm]. The HBV model uses a degree-day approach that, based on air temperature and the water retention capacity of the snow, describes snowmelt (q_m) in [mm] (eq. 3.1) and potential refreezing of melt water (q_r) in [mm] (eq. 3.2).

$$q_m(t) = CFMAX * (T(t) - TT) \quad (3.1)$$

$$q_r(t) = CFR * CFMAX * (TT - T(t)) \quad (3.2)$$

TT	Temperature limit for snow/rain $^{\circ}\text{C}$
$CFMAX$	Degree-day factor of snowmelt $[\text{mm } ^{\circ}\text{C}^{-1} \text{ d}^{-1}]$
CFR	Degree-day factor of refreezing $[\text{mm } ^{\circ}\text{C}^{-1} \text{ d}^{-1}]$

Soil moisture routine

The soil moisture routine accounts for the overall wetness of the catchment. Fluxes into the soil moisture routine are capillary transport (q_c) in [mm] (eq 3.3) from the fast response routine and infiltration from the precipitation routine. The infiltration is further divided into infiltration (q_{in}) in [mm] (eq 3.4) into the soil moisture storage box (S_{sm}) and infiltration (q_d) in [mm] (eq 3.5) that directly feeds into the fast response storage box (S_{sw}).

$$q_c(t) = CFLUX * \frac{FC - S_{sm}(t)}{FC} \quad (3.3)$$

$CFLUX$	Maximum rate of capillary flow $[\text{mm } \text{d}^{-1}]$
---------	---

$$q_{in}(t) = S_{mw}(t) + q_m(t) + P_r(t) - q_r(t) - WHC * S_{sp}(t) \quad (3.4)$$

$$q_d(t) = q_{in}(t) + S_{sm}(t) - FC \quad (3.5)$$

WHC Water Holding Capacity of snow [-]
FC Maximum soil moisture content [mm]

Outgoing fluxes from the soil moisture storage are the evapotranspiration (et_a) in [mm] (eq 3.6) and seepage (q_s) in [mm] (eq 3.7) into the fast response routine storage

$$et_a(t) = et_p(t) * \frac{S_{sm}(t)}{LP * FC} \quad \text{if } S_{sm}(t) < LP * FC \quad (3.6)$$

$$et_a = et_p(t) \quad \text{if } S_{sm}(t) \geq LP * FC$$

$$q_s = \left(\frac{S_{sm}(t)}{FC} \right)^\beta * (q_{in}(t) - q_d(t)) \quad (3.7)$$

et_p Model input, a time series containing the potential evapotranspiration [mm]
 β Soil routine parameter [-]
 LP Limit for potential evapotranspiration [-]

Fast runoff response routine

The fast runoff response routine has one storage box (S_{sw}) with five fluxes connected to it. Incoming fluxes are the previously mentioned direct runoff and seepage. Outgoing fluxes are the previously mentioned capillary rise, percolation (q_{perc}) in [mm] to the slow runoff response routine and fast runoff q_f in [mm] (eq 3.8)

$$q_f(t) = KF * S_{sw}(t)^{1+\alpha} \quad (3.8)$$

KF Recession coefficient of the fast runoff response reservoir [d^{-1}]
 α Response box parameter [-]

Percolation to the slow runoff response box is not described by an equation but is expressed by parameter *PERC* describing the amount of water in [mm] that will percolate from the fast runoff response routine storage to the slow runoff response routine storage S_{gw} .

Slow runoff response routine

The slow runoff response routine has one reservoir S_{gw} with one inflow and one outflow. The only inflow into the slow routine is the previously described percolation from the fast runoff response reservoir. The only outflow is the slow runoff q_s [mm] (eq 3.9).

$$q_s(t) = KS * S_{gw}(t) \quad (3.9)$$

KS Recession coefficient of the slow runoff response reservoir [d^{-1}]

3.2 SENSITIVITY ANALYSIS

The HBV model uses 14 parameters in the model routines to translate the model inputs to a runoff value. A risk of a high number of model parameters is that it might result in different parameter sets resulting in a similar model performance, an issue also often referred to as overparameterization (Booij, 2005). To reduce the number of model parameters to be calibrated in the calibration procedure a sensitivity analysis will be applied. The sensitivity analysis will indicate which parameters are most influential for the model performance and should be considered in the model calibration (Song et al., 2015).

Measures to assess the performance of a model are found in objective functions. These objective functions give a quantification of how well the model output corresponds to observations. Different objective functions emphasize different parts of the hydrograph. The objective functions that will be used in this research will be described in section 3.2.1. Section 3.2.2 will be used to elaborate on the sensitivity analysis method.

3.2.1 OBJECTIVE FUNCTIONS

Objective functions are used to quantify the quality at which model output resembles the observations. Multiple objective functions are available for this assessment of the goodness of fit. These different objective functions all use different mathematical functions to quantify the quality of the simulations when compared to observations. These differences allow for the different objective functions to focus on different parts of the hydrograph (e.g. peak flows, periods of low flow). Cheng (2014) presents an overview of classical objective functions that are regularly used in hydrological modelling studies.

The objective of this research is to find whether there is a trade-off between using different objective functions in model calibration when the aim is to not only simulate the total runoff correctly but also the runoff components. To find this trade-off between objective functions, a weighted combination of two objective functions will be used. From the two objective functions that will be selected, one objective function will put more emphasis on high flow and the other objective function will emphasize low flows. The objective functions that have been selected for this purpose are the Nash-Sutcliffe efficiency criterion (NS) (Nash & Sutcliffe, 1970) and the logarithmically transformed Nash-Sutcliffe efficiency criterion (NSL) (Krause et al., 2005). The NS has been selected because fast runoff has a large contribution to the total runoff during periods of high runoff and runoff peaks, the part of the hydrograph on which the NS puts more emphasis. The NSL on the other hand emphasises periods of low flow more, during these periods baseflow is the dominant runoff component.

NS is an objective function that is often used in hydrological modelling studies (e.g. Swamy & Brivio, 1997; Wu & Xu, 2006; Lemonds & McCray, 2007; Benninga et al., 2017; Romanowicz et al., 2016; Osuch et al., 2017). The so-called efficiency that quantifies the quality of the simulation is calculated according to equation 3.10:

$$NS = 1 - \frac{\sum_{i=1}^{i=n} (Q_{obs,i} - Q_{sim,i})^2}{\sum_{i=1}^{i=n} (Q_{obs,i} - \overline{Q_{obs}})^2} \quad (3.10)$$

Where $Q_{obs,i}$ denotes the observed discharge at time step i , $Q_{sim,i}$ denotes the simulated discharge at time step i and $\overline{Q_{obs}}$ is the mean observed discharge. The NS is defined as one minus the sum of the differences between the model output and observations squared and normalized by dividing by the variance of the observations from the considered time period. The value that NS can assume ranges from $-\infty$ to 1 where a NS value of 1 indicates that the simulated discharge exactly agrees with the observed discharge at every time step. Values less than 1 indicate that

differences between the observed and simulated discharges exist with lower values indicating larger discrepancies between the model output and the observations.

Because the NS uses the sum of the differences squared this objective function is more sensitive to high flows. This is a valuable property for assessing the correctness at which peak flows are simulated but can be a limitation when assessing the goodness of the simulation of low flows or baseflow.

An objective function that puts more emphasis on low flows is the logarithmically transformed NS (NSL) (Cheng, 2014). Prior to assessing the goodness of the simulation, the observed and modelled hydrographs are logarithmically transformed (eq. 3.11). Following the same methodology as the NS for assessing the correctness of the simulation, this method places more emphasis on low flows compared to the NS (Tesemma et al., 2014). Krause et al. (2015) also presents the NSL as an efficiency criterion that is especially suited for assessing periods of low flow because the influence of high flow values is greatly reduced.

$$NSL = 1 - \frac{\sum_{i=1}^{i=n} (\log(Q_{obs,i}) - \log(Q_{sim,i}))^2}{\sum_{i=1}^{i=n} (\log(Q_{obs,i}) - \log(\overline{Q_{obs}}))^2} \quad (3.11)$$

3.2.2 SOBOL'S METHOD

A broad palette of methods is available for sensitivity analyses all of different complexities and based on different underlying assumptions on how to correctly assess parameter sensitivity (Song et al., 2005). This can lead to different methods resulting in different results when ranking the parameters based on their relative importance (Frey & Patil, 2002).

Sobol's method for global sensitivity analysis is considered as one of the more robust methods available (Tang et al., 2007). Also, the Sobol method does not rely on model structure or assumptions about the model functioning, e.g. linearity or additivity of the model (Saltelli et al., 2000). The method is classified as a variance decomposition method and results in the overall parameter sensitivity as well as the variance explained by interactions between parameters (Homma & Saltelli, 1996). The goal of this sensitivity analysis is to quantify the contribution of each parameter to the total variance in the model output. This allows the modeler to exclude insensitive parameters from the model calibration by fixing them at a set (default) value (Saltelli et al., 2000).

The contribution of variance to the model output by a parameter X_i consists of the main effect, V_i , and the total effect, V_{Ti} (Saltelli et al., 2004). These effects are defined by Saltelli et al. (2004) as follows (eq. 3.12 and eq. 3.13):

$$V_i = V[E(Y|X_i)] \quad (3.12)$$

$$V_{Ti} = V[E(Y|X_{-i})] \quad (3.13)$$

V_i indicates the amount of variance that is contributed to the model result if the true value of only parameter X_i was known and the other parameters were allowed to vary. The total effect, V_{Ti} , indicates how much of the variance is left unexplained if the exact values of all the parameters except X_i were known.

The sensitivity of the parameters can be found by dividing the two variance components by the total output variance $V(Y)$ (eq. 3.14 and eq. 3.15). Where S_i is the sensitivity to first order term and S_{Ti} denotes the total sensitivity index which is a summation of the main effect and interactions with other parameters. The influence of the interactions between parameters on the output sensitivity is determined according to equation 3.16.

$$S_i = \frac{V[E(Y|X_i)]}{V(Y)} \quad (3.14)$$

$$S_{Ti} = \frac{E[V(Y|X_{-i})]}{V(Y)} \quad (3.15)$$

$$S_{interaction} = S_{Ti} - S_i \quad (3.16)$$

A sensitivity analysis package was provided by the Polish Academy of Sciences, Institute of Geophysics which, among others, included the Sobol method. The Sobol sensitivity analysis was run for all three catchments for both the NS and the NSL objective functions (section 3.3.2). Every simulation was run using 30 000 samples and used the 30 years of the observational data covering the years 1976 until 2005 that will also be used for model calibration. This resulted in sensitivity indices for all 14 parameters in every catchment for both the objective functions.

Determining appropriate thresholds above which parameters are considered for model calibration and below which parameters will be set to a default value is generally an arbitrary decision (e.g. Bastidas et al., 1999; Tang et al., 2007; Knoben, 2013). Here, similarly, the decision on which parameters to include in the model calibration and which ones to fix at a default value will be a subjective one.

Using the outcomes of the sensitivity analysis we can classify the model parameters in three main groups based on the amount of variance they explain and therefore also their necessity to be calibrated:

- Parameters that have a high main effect: these parameters influence the overall model performance independently of interaction with other model parameters;
- Parameters that have a small main effect but a high total effect: these model parameters mainly influence the model performance through interactions with other parameters;
- Parameters that display a small main effect and a small total effect: these parameters have a negligible effect on the overall model performance and freezing these parameters to their default value is justified (Saltelli et al., 2004).

It is aimed to reduce the number of model parameters that will be calibrated to 8 by taking the parameters that displayed the highest sensitivity from the sensitivity analysis. The choice on which parameters to include will be made based on the total sensitivity index.

3.3 MODEL CALIBRATION

In this chapter the approach that is taken to calibrate the HBV model is presented. Firstly, the choice on which calibration algorithm will be applied is presented in section 3.1.1. The calibration algorithm that is decided on and will be applied in this research is presented in section 3.3.2 and the periods that will be used for model calibration and validation presented in section 3.3.3.

3.3.1 CALIBRATION ALGORITHM CHOICE

During the calibration procedure the aim is to find the parameter set that allows the model to generate a model output that resembles the observations as closely as possible. To find this parameter set, the Shuffled Complex Evolution Metropolis (SCEM-UA) calibration algorithm will be used (Vrugt et al., 2003a). The SCEM-UA algorithm is a further development of the work of Duan et al. (1992) who presented the SCE-UA algorithm for calibration (of conceptual rainfall-runoff models). The SCE-UA algorithm combines elements from several optimization strategies into one algorithm. Numerous case studies have demonstrated the robustness and efficiency of the SCE-UA algorithm in finding the global optimum. The difficulty for the SCE-UA algorithm is identifying a unique best parameter set that performs significantly better than other feasible parameter sets in its proximity (Vrugt et al., 2003b). Calibration of the HBV model will be done by using the precipitation, the potential evapotranspiration and the temperature observations as model inputs. The model outputs will be evaluated against the discharge observations by using the objective functions described earlier in section 3.2.1.

To be able to identify a trade-off between the two objective functions (section 3.2.1), weights will be assigned to both the objective functions during the model calibration. The weights assigned to both objective functions are varied from 0% to 100% with increments of 10% while keeping the sum of the weights equal to 100%. For each of the combination of weights assigned to the objective functions an optimum parameter set will be found resulting in a total of 11 best performing parameter sets per catchment.

Before calibration of the HBV model will be done an exploratory Monte Carlo (MC) analysis will be done to determine the appropriate parameter ranges. The parameters that will not be considered in the calibration have been set to their default values according to the HBV manual version 5.10 (SMHI, 2006). For the parameters that will be calibrated preliminary parameter ranges are adopted from Benninga (2017) and Osuch et al. (2016). In the MC analysis the performance of 250 000 parameter sets will be evaluated where each parameter that will be calibrated is individually sampled from a uniform distribution. For each sample the NS and NSL values are then calculated from the output of the HBV model. By evaluating how individual parameter values from the MC samples relate to NS and NSL achieved by the according parameter set, parameter ranges can be adjusted to more appropriate ranges whilst still taking into account their physical meaning and interpretation

3.3.2 CALIBRATION ALGORITHM

The SCEM-UA algorithm applies Markov Chain Monte Carlo (MCMC) sampling following the Metropolis Hastings (Metropolis et al., 1953) strategy instead of the Downhill Simplex procedure, used in the SCE-UA algorithm, for evolution of the population. This change allows the algorithm to find the most likely parameter set as well as its posterior probability distribution. Vrugt et al. (2003a) describe the steps that are involved in the process of finding the 'best' parameter set. From the feasible parameter space bounded by the parameter minimum and maximum values, the SCEM-UA algorithm randomly draws the initial population and ranks the sample points in descending posterior density. These initial sample points also serve as the initial points from where the parallel chains will start to evolve. Proposal points for evolving the chain into the next generation are drawn from the proposal distribution that corresponds to the individual chain. The posterior distributions of the new generations are then evaluated and can be either accepted or rejected. If the proposed evolution is accepted the chain then progresses to the new

position. If the proposed evolution is not accepted the chain remains at the current position. After every evolution it is checked for convergence according to the Gelman Rubin convergence statistic (Gelman & Rubin, 1992). The calibration process is terminated if either the Gelman Rubin convergence criteria is satisfied or if the predefined maximum number of iterations has been executed. The default settings for the SCEM-UA algorithm are adopted from Vrugt et al. (2003b) and are presented in Table 3-1.

TABLE 3-1: SCEM-UA ALGORITHM PARAMETERS (VRUGT ET AL., 2003B)

Setting	Description	Value
nSamples	Population size	200
nCompl	The number of complexes	5
nModelEvalsMax	The maximum number of model iterations	10 000
drawInterval	Shuffling rate of complexes	5

3.3.3 CALIBRATION AND VALIDATION PERIOD

The provided datasets by the IGF PAN consist of 40 years of continuous observations spanning from 1 January 1971 until 31 October 2010. The dataset is used for two purposes, namely: (1) calibration of the HBV model and (2) validation of the HBV model. To prevent biased results periods have been defined that do not overlap.

Model calibration using the SCEM-UA algorithm will be done using the observations between 1 November 1976 and 31 October 2005. The validation of the model calibration will be done by applying a split-sample test (Klemeš, 1986). The split-sample test will be done using the observational data from 1 November 2005 until 31 October 2010.

3.4 SIMULATION OF RUNOFF COMPONENTS

There is widespread agreement that for assessing model performance the correspondence between the total measured and modelled stream flow is not a sufficient indicator. Additional insights in the processes that take place within the catchment would be a step towards improvement of runoff modelling (Beven, 1989). Yet, in most cases the assessment of model performance is still done based on the total runoff because individual components that contribute to the total runoff usually go unobserved. The information that observed hydrographs provide however, is not limited to the absolute values of the measured runoff. Eckhardt et al. (2002) presents an example of what the potential benefits of having insight in the runoff components can provide for model performance.

3.4.1 HYDROGRAPH SEPARATION

Over the years, many methods have been developed that allow for the identification of the baseflow component from the total runoff e.g. low-pass filtering, recursive filtering and unit hydrograph methods. Often linear reservoirs have been used for modelling the groundwater contribution, i.e. baseflow, to the total flow (e.g. Chapman, 1999; Fenicia et al., 2006; Eckhardt, 2005). More recent studies however by Wittenberg (1994, 1999, 2003), Gan & Luo (2013) and Aksoy et al., (2008) have used nonlinear reservoirs for the analysis of groundwater recession and baseflow contribution as these methods appeared to give a more realistic representation of catchment processes. Baseflow separation in this research is done according to the non-linear reservoir approach from Wittenberg (1999).

Wittenberg's baseflow separation method assumes a power-law relationship between the baseflow and the groundwater storage of the catchment (eq. 3.17). With S denoting the groundwater storage and Q representing the recession of the baseflow and a and b are model parameters. Parameters a and b for flow recessions are found by an iterative process by calibrating them against flow recession data by utilizing a least-squares method (Wittenberg, 1999).

$$S = a * Q^b \quad (3.17)$$

The analytical solution for the baseflow is presented by Wittenberg (1999) and is given in equation 3.18. Here Q_B indicates the baseflow resulting from the nonlinear reservoir at time step t starting from initial discharge Q_0 .

$$Q_B = Q_0 \left[1 + \frac{(1-b) * Q_0^{1-b}}{ab} * t \right]^{\frac{1}{b-1}} \quad (3.18)$$

With the contribution of the baseflow to the total flow determined by applying Wittenberg's baseflow separation method the fast runoff (Q_F) component can easily be found by subtracting the baseflow component from the total flow (Q_T) (eq. 3.19).

$$Q_F = Q_T - Q_B \quad (3.19)$$

To illustrate the results of the hydrograph separation the hydrograph separation done for the Biała Tarnowska catchment for the year 1976 is graphed and presented in Figure 3-3. It shows that during periods of low flow the runoff almost entirely consists of baseflow and that fast runoff barely contributes to the total runoff. During high runoff events it is observed that the baseflow also increases but the main contribution to the total flow becomes the fast runoff component.

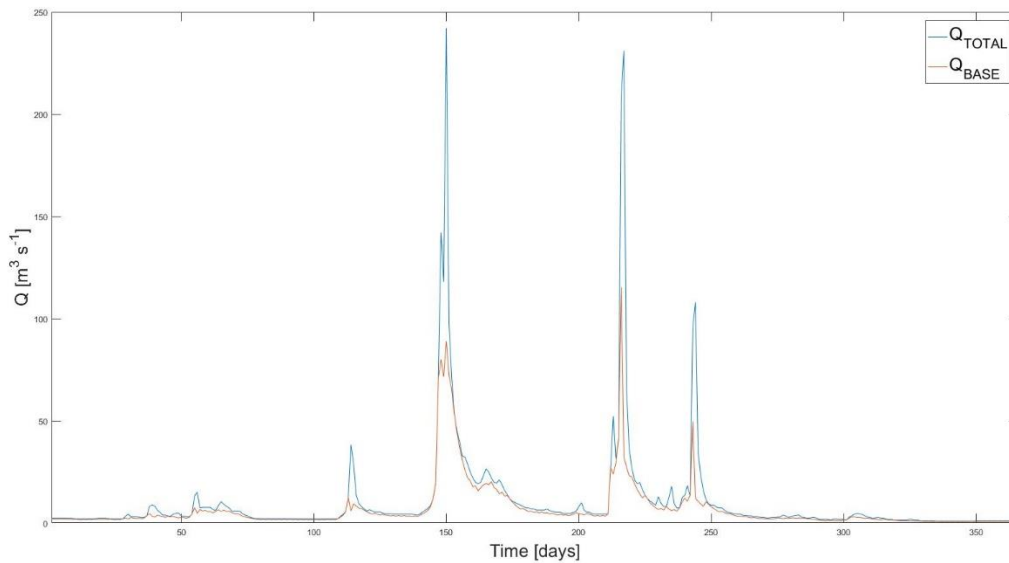


FIGURE 3-3: WITTENBERG'S BASEFLOW SEPARATION APPLIED TO THE BIALA TARNOWSKA CATCHMENT FOR THE YEAR 1976

3.4.2 SIMULATION OF RUNOFF COMPONENTS

Determining model performance in simulating the runoff components will be done by comparing the runoff components derived from the observed runoff for the calibration period with the runoff components derived from the simulated runoff for the calibration period. This is done for each simulation using the different parameter sets that resulted from model calibration (section 3.3). Assessing the correctness of the simulated runoff components for the previously determined parameter sets will be done by using the previously described NS objective function (section 3.2.1).

Identifying a trade-off between using different objective functions and the model its ability to correctly simulate the runoff components will be done by checking if there is a correlation between the weights assigned to the objective

functions and the correctness at which the individual runoff components are simulated. The determined correlation will be checked for statistical significance using a two-sided test at a significance level of $\alpha = 0.10$.

3.5 CLIMATE CHANGE IMPACT

For assessing the impact that projected climate change will have the HBV model will be forced with the climate data from the seven GCM/RCM combinations. From the seven resulting time it will be assessed what the impact of climate change will be for the total runoff from the catchments. For each catchment the mean annual runoff will be presented along for the projected changes to the mean annual runoff from the catchments.

Secondly impacts of projected changes on the flow components will be researched. This will be done by comparing the future contributions of the flow components with the contributions of the flow components to the total flow in the predefined reference period. For this comparison the following periods are defined: the reference period 1976-2005, the near-future 2021-2050 and the far-future 2071-2100. Unique parameter sets will be found for the Wittenberg filter for each period in order to obtain most realistic separation in runoff components for the individual periods. By using 30-year periods this problem is dealt with because over the shorter 30-year periods it is assumed that the parameters are roughly stationary and unique parameter sets will be found for each period. The goal of this comparison is to indicate if one runoff component is projected to become more dominant in the future and flow composition is projected to change.

In addition to assessing the contribution of the flow components on an annual time scale the contributions of the runoff components to the total flow will be assessed at a seasonal scale. Federer (1973) and Weisman (1977) both describe seasonal variability in the stream flow formation and attribute this to evapotranspirational losses from the catchment. From the climate change projections, it is already known that the temperatures are projected to increase in the three considered catchments, thus also increasing the potential evapotranspiration. By assessing the runoff components on a shorter time scale seasonal variability in the contributions of the components can be identified. Doing so allows to identify possible trends between the reference period, the near-future and far-future in the seasonal contributions of the runoff components.

Lastly the impacts of projected climate change on the low flows will be assessed. As described in section 3.4.1, during periods of low flow the runoff almost entirely consists of baseflow so this approach to looking at climate change impacts aims to identify what changes the baseflow might undergo during periods of extended drought. To assess the impact of projected climate change on this part of the hydrograph the changes in the 90th percentile (Q90) of the flow will be assessed. The Q90 is a commonly used indicator to assess low flows in hydrographs and indicates the flow threshold that is exceeded 90% of the time (e.g. Ward, 2007; Gorgen et al., 2010; Hatterman et al., 2017). For this purpose, the Q90 that is derived from the reference period will be compared to the Q90 that is derived from the near-future and far-future periods to indicate if the Q90 is projected to change.

4 RESULTS

In this chapter the results that are obtained from this research are presented and discussed. Section 4.1 will be used to present the results from the sensitivity analysis, followed by the results obtained for model calibration and validation in section 4.2. How well the runoff components are simulated is evaluated in section 4.3 and trade-offs that are identified between the objective functions are presented in section 4.4. This chapter is concluded with the impacts of projected climate change in section 4.5.

4.1 SENSITIVITY ANALYSIS

In figures 4-1, 4-2 and 4-3 the results from the variance decomposition are presented as bar plots. For each catchment the sensitivity to every parameter is displayed. The total sensitivity index is presented as well as the main effect and the influence of interactions with other parameters which together make up the total sensitivity.

Following from this sensitivity analysis is a quantification of the influence of the model parameters on the model output variance according to the NS objective function. Parameters that appear to largely contribute to the model output variance are parameters that are part of the soil moisture routine and the fast runoff routine (FC, BETA, LP, ALFA, KF and PERC). This is not surprising because the NS emphasizes peak flows to which the fast runoff contributes significantly (Blume et al., 2007).

As for the sensitivity when using the NSL as objective function the KS TT, CFMAX and WHC parameters appear prominently in the results for all three catchments. From these parameters KS is related to the lower response box from HBV that represents the slow runoff. Parameters TT, CFMAX and WHC are part of the snow module that can be responsible for delaying runoff depending on the temperature. Precipitation that falls in the form of snow is therefore often not discharged as a runoff peak but rather at a more constant rate. Because of this sensitivity towards the NS is low but it displays higher sensitivity towards the NSL.

The sensitivity analysis indicates that some parameters show a small negative sensitivity which should not be possible. Saltelli et al. (2004) describes that these negative values are explained by numerical errors in the Sobol method and are not uncommon when sensitivity indices have a value of approximately zero. The probability of encountering negative values as outcome from the analysis can be reduced by increasing the sample size. Because the negative values that are found are very small it is accepted that these values are rounded to zero.

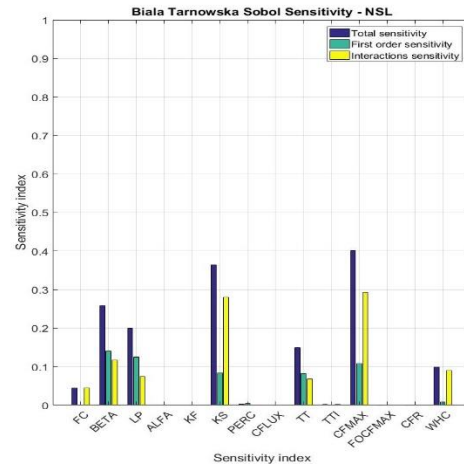
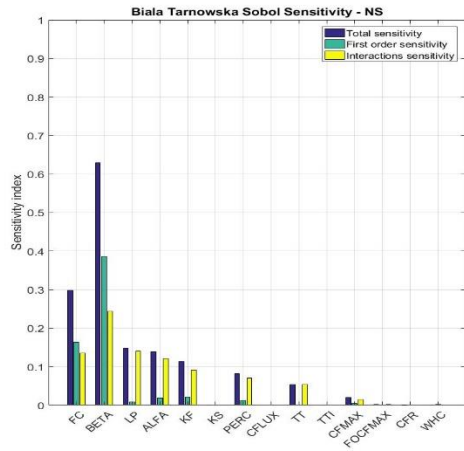


FIGURE 4-1: RESULTS OF VARIANCE DECOMPOSITION FOR THE BIAŁA TARNOWSKA CATCHMENT

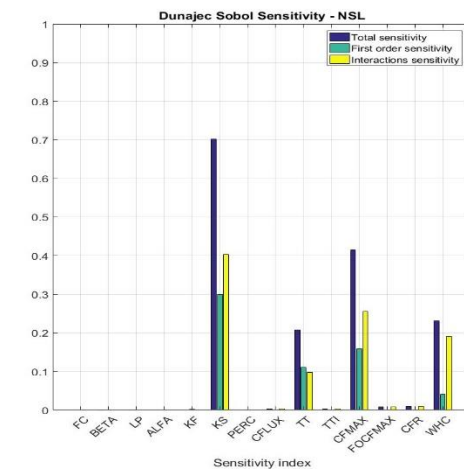
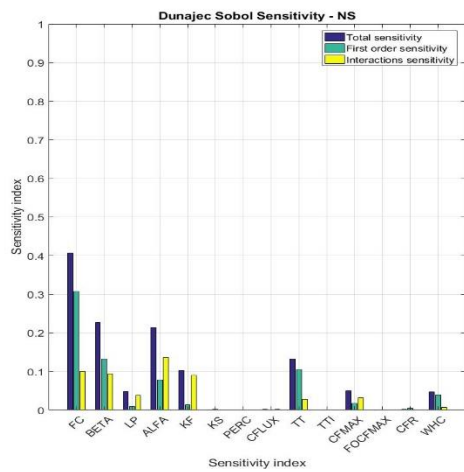


FIGURE 4-2: RESULTS OF VARIANCE DECOMPOSITION FOR THE DUNAJEC CATCHMENT

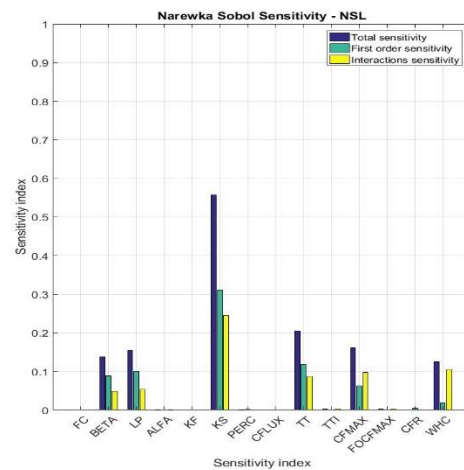
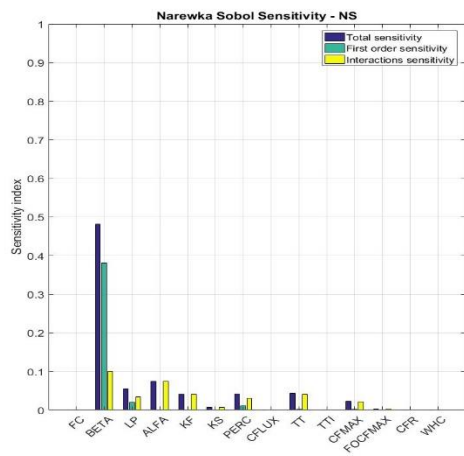


FIGURE 4-3: RESULTS OF VARIANCE DECOMPOSITION FOR THE NAREWKA CATCHMENT

It was aimed to reduce the number of parameters to 8 whilst taking an equal number of parameters from the sensitivity analysis towards the NS as the sensitivity analysis towards the NSL. The choice on which parameters to include was made based on the total sensitivity index. Parameters that will be considered in the model calibration are presented in Table 4-1.

TABLE 4-1: HBV MODEL PARAMETERS THAT WILL BE TAKEN INTO ACCOUNT FOR MODEL CALIBRATION PER CATCHMENT

Biała Tarnowska	Dunajec	Narewka
FC	FC	BETA
BETA	BETA	LP
LP	ALFA	ALFA
ALFA	KF	KF
KF	KS	KS
KS	TT	TT
TT	CFMAX	CFMAX
CFMAX	WHC	WHC

4.2 MODEL CALIBRATION

In this section the results from model calibration and intermittent steps will be presented. Firstly, the results from the exploratory Monte Carlo simulation are presented in section 4.2.1 followed by the results of the model calibration in section 4.2.2.

4.2.1 PARAMETER RANGES

For every parameter the sampled value for each simulation is plotted against the NS and NSL score. These plots are presented in appendix A (figures A-1, A-2 and A-3). These plots show how the NS and NSL scores are distributed over the preliminary parameter range for each sampled parameter. These plots are then used as an indicator according to which the parameter ranges can be adjusted such that it encapsulates the range in which the best simulation results are found according to both the NS and the NSL scores and excludes the parameter range where low scores are obtained for both the NS and the NSL. Similarly, the parameter ranges can be extended further if the simulations indicate a clustering of best simulations near the edge of a parameter range and if the physical interpretation of the parameter is not violated. In tables 4-2, 4-3 and 4-4 the definitive parameter ranges are presented for the Biała Tarnowska, Dunajec and Narewka catchments. Additionally, in Table 4-5 the default parameter values are presented for the HBV model that are used for parameters that will not be considered in model calibration. These default values are adopted from the HBV manual (SMHI, 2006).

TABLE 4-2: DEFINITIVE PARAMETER RANGES USED IN CALIBRATION OF THE HBV MODEL FOR THE BIAŁA TARNOWSKA CATCHMENT

Parameter	Unit	Minimum value	Maximum value
FC	mm	0.1	500.0
BETA	-	0.01	5.00
LP	-	0.10	1.00
ALFA	-	0.10	1.50
KF	d ⁻¹	0.0005	0.20
KS	d ⁻¹	0.0005	0.20
TT	°C	-1.00	3.00
CFMAX	mm d ⁻¹	0.00	20.00

TABLE 4-3: DEFINITIVE PARAMETER RANGES USED IN CALIBRATION OF THE HBV MODEL FOR THE DUNAJEC CATCHMENT

Parameter	Unit	Minimum value	Maximum value
FC	mm	0.1	1000.0
BETA	-	0.01	7.00
ALFA	-	0.10	1.50
KF	d ⁻¹	0.0005	0.10
KS	d ⁻¹	0.0005	0.30
TT	°C	-3.00	1.00
CFMAX	mm d ⁻¹	0.00	10.00
WHC	mm mm ⁻¹	0.00	1.00

TABLE 4-4: DEFINITIVE PARAMETER RANGES USED IN CALIBRATION OF THE HBV MODEL FOR THE NAREWKA CATCHMENT

Parameter	Unit	Minimum value	Maximum value
BETA	-	0.01	4.50
LP	-	0.10	1.00
ALFA	-	0.10	1.50
KF	d ⁻¹	0.0005	0.20
KS	d ⁻¹	0.0005	0.20
TT	°C	-3.00	2.00
CFMAX	mm d ⁻¹	0.00	20.00
WHC	mm mm ⁻¹	0.00	1.00

TABLE 4-5: DEFAULT PARAMETER VALUES FOR THE HBV MODEL (SMHI, 2006)

Parameter	Unit	Default parameter value
FC	mm	200.0
LP	-	0.90
CFLUX	mm d ⁻¹	1.00
TTI	°C	0.00
FOCFMAX	-	1.00
CFR	-	0.05
WHC	mm mm ⁻¹	0.10

4.2.2 CALIBRATION RESULTS

Calibration of the HBV model for the Biała Tarnowska, Dunajec and the Narewka catchments resulted in 11 best parameter sets for each catchment, each corresponding to a combination of NS and NSL weights. The NS and NSL scores obtained with each parameter set are presented below separately for each catchment. The decision on which parameter set will be used for assessment of climate change impact will be discussed separately in section 4.4.

Biała Tarnowska

For the 11 different combinations of NS and NSL weights that have been used in the calibration procedure, the calibration results are presented in Figure 4-4. The results show that the NSL performance criteria shows a substantially lower model performance than the NS does for all combinations of weights.

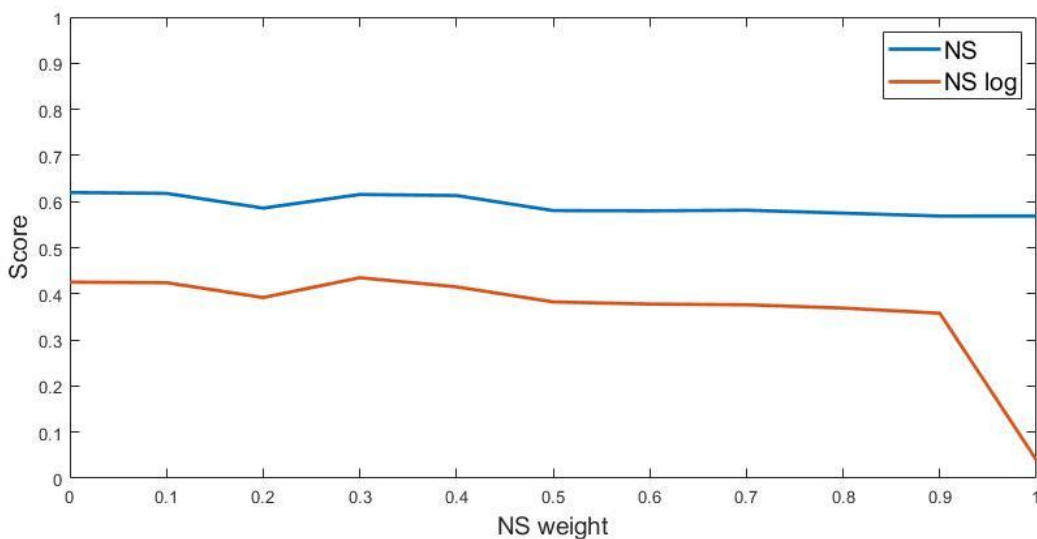


FIGURE 4-4: CALIBRATION RESULTS FOR THE BIAŁA TARNOWSKA CATCHMENT

Model performance with the parameter sets that were found during the calibration procedure appears to be low when compared to previous hydrological modelling research on the Biała Tarnowska catchment (e.g. Benninga et al., 2017; Osuch et al., 2016). Using the DEGL calibration algorithm and NS objective function to calibrate the HBV model, Benninga (2017) found a parameter set that achieved NS scores of 0.78 and 0.74 for the calibration and validation respectively for the Biała Tarnowska catchment. The parameter set found by Osuch et al. (2016) for the HBV model achieved NS scores of 0.77 and 0.80 for the calibration and validation periods respectively. The NS scores that are found when exclusively the NS is used for model calibration are 0.57 and 0.55 for model calibration and validation respectively.

It must be noted that these researches both used a different calibration period than was used in this research which might have negatively impacted the obtained calibration and validation results despite the periods having a large overlap with the calibration period used in this research. Both Benninga (2017) and Osuch et al. (2016) used the period spanning from 1971 until 2000 for model calibration whereas this research used the observations from the 1976-2005 period for model calibration. Also, Benninga (2017) applied a different calibration algorithm to optimize the model parameters which might influence the results from model calibration.

Dunajec

The performance of the parameter sets that have been obtained from the model calibration is presented in Figure 4-5. The NS and NSL scores show very similar performance for every increment of NS and NSL weights with the NSL scoring slightly higher than the NS score when the NSL is dominant in the model calibration. As expected, the NS score increases when a higher weight is assigned to the NS objective function and the NSL scores decrease.

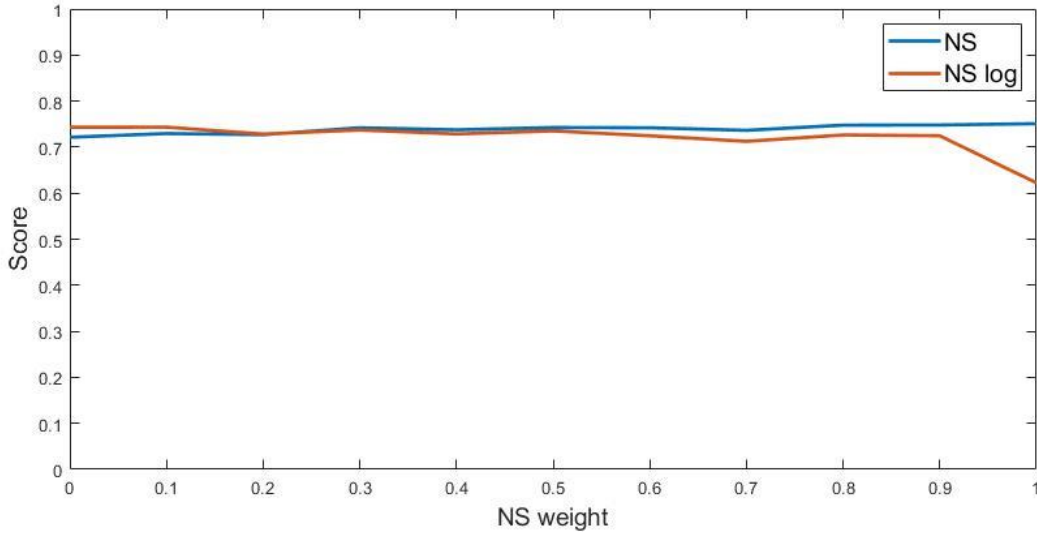


FIGURE 4-5: CALIBRATION RESULTS FOR THE DUNAJEC CATCHMENT

Comparing the model performance with the parameter set that was found by the SCEM-UA algorithm with previously published work on hydrological modelling of the Dunajec catchment shows similar results. The NS scores that are found in this study when exclusively the NS is used for model calibration are 0.75 and 0.77 for model calibration and validation respectively. Osuch et al. (2016) found NS scores of 0.77 and 0.80 for model calibration and validation respectively. Where Osuch et al. again used the years 1971-2000 for model calibration contrary to the 1976-2005 period used in this research.

Narewka

The calibration results of the HBV model for the Narewka catchments are displayed in Figure 4-6 where the NS and NSL scores are presented for every parameter set. The NS and NSL scores show a behaviour similar to the behaviour found in the Dunajec catchment with the NSL scoring being higher than the NS at low NS weights during model calibration but decreasing as the NS weight increases. Additionally, the NS shows the opposite behaviour as expected with the performance increasing as the NS becomes the dominant performance indicator during model calibration.

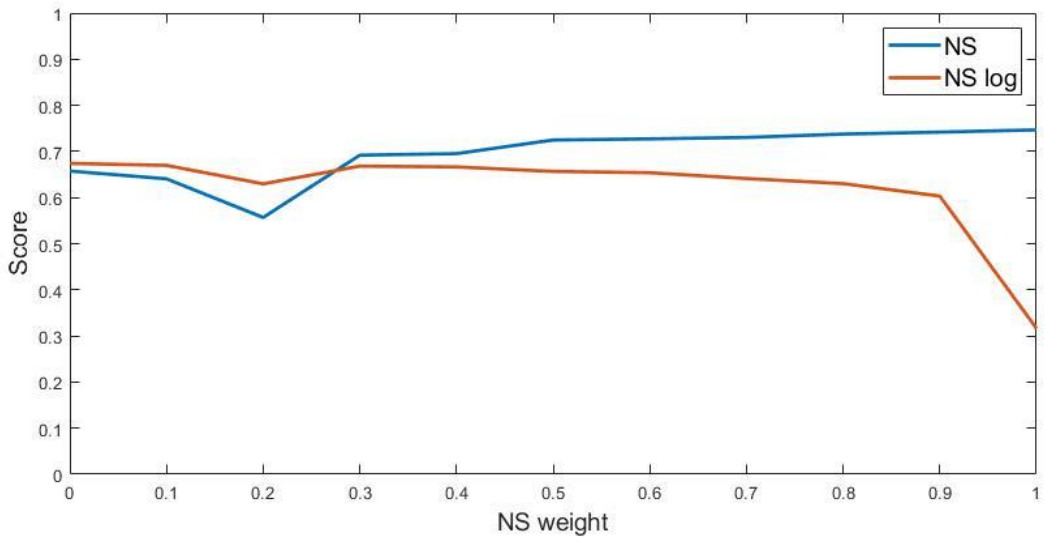


FIGURE 4-6: CALIBRATION RESULTS FOR THE NAREWKA CATCHMENT

This parameter set found when exclusively using the NS as objective function seems to outperform the parameter set found by Osuch et al. (2016) slightly based on the NS as performance indicator. Values found for the NS in the work done by Osuch et al. (2016) are 0.71 for the calibration period and 0.54 for the validation period. Values found for the NS in this study are 0.75 and 0.57 for model calibration and validation respectively.

4.3 SIMULATION OF RUNOFF COMPONENTS

Similar to how the model performance in simulating the total flow was presented in section 4.2.2, the model performance in simulating the individual runoff components is presented. In figures 4-7, 4-8 and 4-9 the NS scores of the fast and slow components are graphed for each catchment. The runoff components are derived from the total runoff using the Wittenberg filter resulting in a fast runoff component and a baseflow component for each simulation.

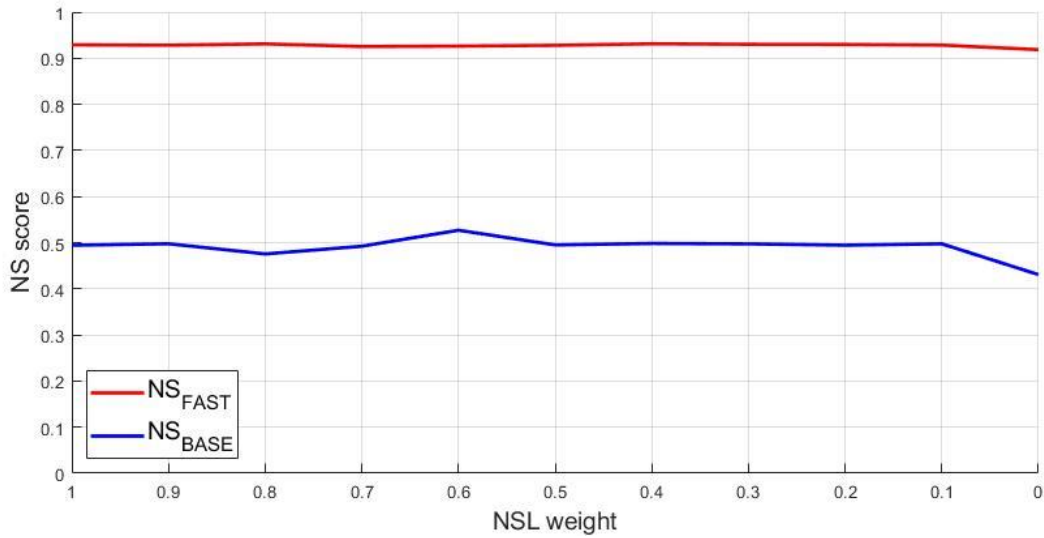


FIGURE 4-7: NS SCORES FOR THE FAST RUNOFF AND BASEFLOW COMPONENTS FOR THE BIAŁA TARNOWSKA CATCHMENT

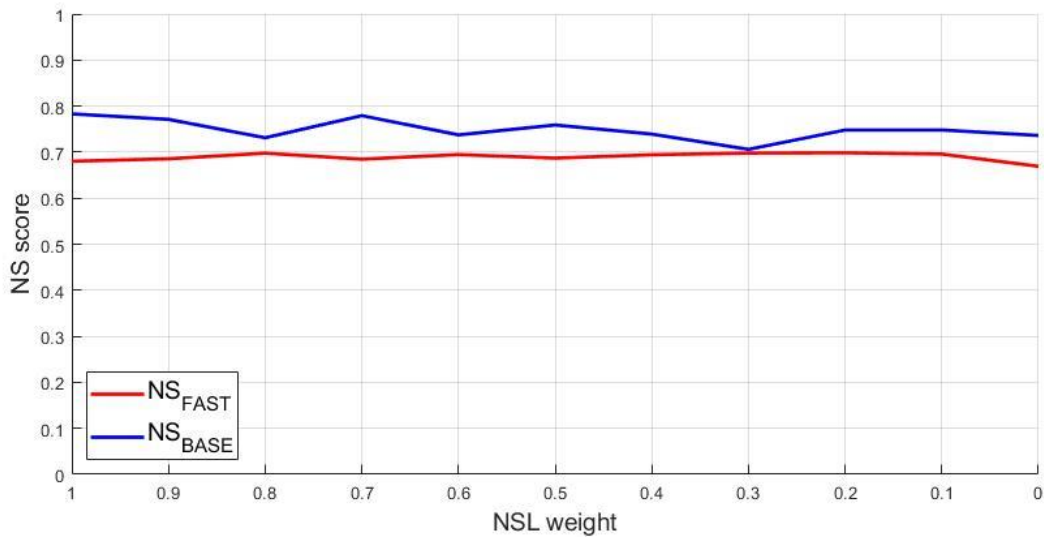


FIGURE 4-8: NS SCORES FOR THE FAST RUNOFF AND BASEFLOW COMPONENTS FOR THE DUNAJEC CATCHMENT

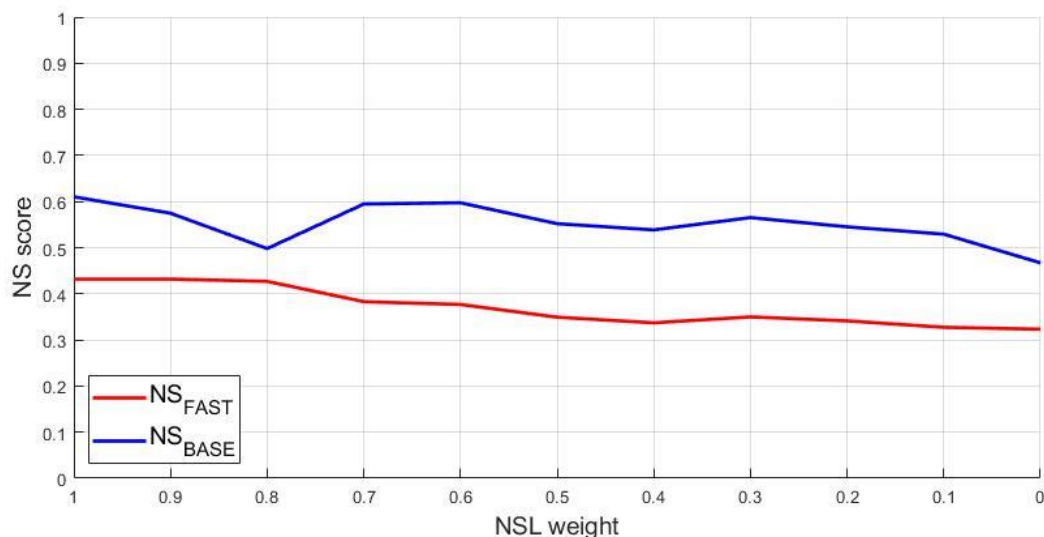


FIGURE 4-9: NS SCORES FOR THE FAST RUNOFF AND BASEFLOW COMPONENTS FOR THE NAREWKA CATCHMENT

For all catchments it can be observed that the correctness at which the components are simulated is, although slightly lower than the correctness of the simulation of the total flow, comparable to how well the total flow is simulated. Because the baseflow and the fast runoff are derived from the total flow by using the Wittenberg method it is expected that a better simulation of the total flow results in a better simulation of the individual runoff components. The obvious outlier however seems the fast component from the Biała Tarnowska catchment, displaying a NS score above 0.9 for all parameter sets indicating a near perfect simulation.

As described in section 3.2.1 the NS objective function is especially sensitive to high flows. It appears that the timing of the runoff peaks of the fast component for the Biała Tarnowska is simulated nearly perfect. Over the period 1976 – 2005 the timing of runoff peaks is on average off by 0.01 to 0.02 time step for the Biała Tarnowska compared to the 0.12 to 0.19 time step for the Dunajec and 0.12 to 0.21 time step for the Narewka catchments. The correct simulation of the timing of the runoff peaks appears to be highly influential for achieving a good simulation of the fast runoff component.

4.4 TRADE-OFF BETWEEN OBJECTIVE FUNCTIONS

For all three catchments the goodness at which the runoff components are simulated have been determined for each of the 11 parameter sets. For each catchment the correlation between the NS of the components (NS_{FAST} and NS_{BASE}) and the NSL weight has been determined. The results are presented below for every catchment in Table 4-6.

TABLE 4-6: CORRELATIONS BETWEEN THE NS SCORES OF THE COMPONENTS AND THE WEIGHT ASSIGNED TO THE NSL

	Correlation coefficient NS _{FAST} and NSL weight	Significant	Correlation coefficient NS _{BASE} and NSL weight	Significant
Biała Tarnowska	0.32	No	0.74	Yes
Dunajec	-0.34	No	0.50	Yes
Narewka	0.94	Yes	0.61	Yes

For the Biała Tarnowska catchment a correlation of 0.32 has been found between the NS_{FAST} and the NSL weight. The correlation that was found between the NS_{BASE} and the NSL weight is 0.74. At the predetermined confidence level (section 3.4.2) these correlations have been checked for statistical significance. The correlation determined between the NS_{FAST} and the NSL weight appeared to be not significant. The correlation between the NS_{BASE} and the NSL weight however is significant. For the Dunajec catchment an insignificant correlation of -0.34 has been found between the NS_{FAST} and the NSL weight. Again, a significant correlation was identified between the NS_{BASE} and the NSL weight with a correlation coefficient of 0.74. The Narewka catchment is the only catchment displaying a significant positive correlation between both the NS_{FAST} and NSL weight and the NS_{BASE} and NSL weight at calculated correlations of 0.94 and 0.61 respectively.

These results display a moderate to strong correlation between the NS_{BASE} and NSL weight for all three catchments, therefore indicating that the best results for modelling baseflow with the HBV model for these catchments will be obtained by using exclusively the NSL as objective function in model calibration. For the fast runoff component however, the results from this study are not unanimous with results from two catchments indicating that there is no correlation between the NS_{FAST} and the NSL weight and only one catchment displaying significant correlation between the NS_{FAST} and the NSL weight.

These significant positive correlations between the NSL weight and the NS scores of the baseflow component show that using a high NSL weight in model calibration allows for the best simulation of the baseflow component. There does not appear to be an unambiguous conclusion that can be drawn from these results on how to improve on the skill at which fast runoff is simulated by using the NS or NSL as objective function in model calibration. For assessing the impact of climate change on the runoff components (section 4.5) the parameter sets that are found with using exclusively the NSL objective function will be utilized. These parameter sets that are found from this calibration are presented in Appendix B.

4.5 CLIMATE CHANGE IMPACT

In this section the climate change impact on the runoff components will be presented. Firstly, it will be validated how well the model performs for the 1976-2005 period by forcing the model with the observed climatological variables as well as with the synthetic climate data from the seven. Next, the impact of climate change on the total flow will be presented in section 4.5.2.

In addition to assessing changes to the total runoff, climate change impact will be assessed by comparing the contributions of the runoff components to the total flow for 30-year periods as described in section 3.5. Runoff contributions for the reference period will be presented as well as projections for the near-future period and the far-future period. Additionally, seasonal variability of the runoff components will be presented along with projected changes herein. This chapter will be concluded with an assessment of climate change impacts on low flows.

4.5.1 MODEL PERFORMANCE ON REFERENCE PERIOD

For the reference period model performance will be assessed by forcing the calibrated model with the observed precipitation and temperature. Model performance will be assessed by looking model its ability to correctly simulate the mean flow over the 1976-2005 period. Additionally, the performance of the model, forced with the synthetic climate data from the seven GCM/RCM combinations, will be assessed for this performance indicator. In tables 4-7, 4-8 and 4-9 the mean flow that is obtained from observations and simulations is presented. The numbering of GCM/RCM combinations in these tables corresponds to the numbering as used in section 2.3 where the GCM/RCM combinations are presented.

TABLE 4-7: MEAN RUNOFF FROM THE BIAŁA TARNOWSKA CATCHMENT PER GCM/RCM COMBINATION AND DEVIATION FROM THE OBSERVATED MEAN RUNOFF

	$Q_{\text{mean}} [\text{m}^3 \text{s}^{-1}]$	ΔQ_{mean}
Observed mean flow	9.2	-
Simulation forced with observed climate data	8.5	-7.7%
GCM/RCM 1	8.4	-8.6%
GCM/RCM 2	8.2	-11.2%
GCM/RCM 3	8.9	-3.2%
GCM/RCM 4	8.6	-6.2%
GCM/RCM 5	8.3	-9.6%
GCM/RCM 6	8.8	-4.7%
GCM/RCM 7	7.8	-15.2%
GCM/RCM mean	8.4	-8.4%

TABLE 4-8: MEAN RUNOFF FROM THE DUNAJEC CATCHMENT PER GCM/RCM COMBINATIONS AND DEVIATION FROM THE OBSERVED MEAN RUNOFF

	$Q_{\text{mean}} [\text{m}^3 \text{s}^{-1}]$	ΔQ_{mean}
Observed mean flow	14.2	-
Simulation forced with observed climate data	11.2	-21.1%
GCM/RCM 1	12.0	-15.3%
GCM/RCM 2	11.0	-22.4%
GCM/RCM 3	11.9	-15.8%
GCM/RCM 4	11.9	-15.7%
GCM/RCM 5	11.4	-19.1%
GCM/RCM 6	11.9	-16.0%
GCM/RCM 7	11.0	-22.5%
GCM/RCM mean	11.6	-18.1%

TABLE 4-9: MEAN RUNOFF FROM THE NAREWKA CATCHMENT PER GCM/RCM COMBINATIONS AND DEVIATION FROM THE OBSERVED MEAN RUNOFF

	$Q_{\text{mean}} [\text{m}^3 \text{s}^{-1}]$	ΔQ_{mean}
Observed mean flow	3.3	-
Simulation forced with observed climate data	3.1	-6.1%
GCM/RCM 1	3.2	-3.5%
GCM/RCM 2	3.2	-2.9%
GCM/RCM 3	3.4	2.1%
GCM/RCM 4	3.3	-1.0%
GCM/RCM 5	3.3	-0.6%
GCM/RCM 6	3.4	3.5%
GCM/RCM 7	3.2	-2.0%
GCM/RCM mean	3.3	-0.6%

It is observed that for every catchment the calibrated model that is forced with observed climate data underestimates the runoff from the catchments. Similarly, the HBV model tends to underestimate the flow when forced with synthetic climate data compared to the observed runoff in the 1965-2005 period. For the Biała Tarnowska catchment these underestimations range from -15.2% to -3.2% with an average underestimation of -8.4% for the 7 GCM/RCM combinations. For the Dunajec catchment these underestimations are even larger with underestimations of the flow ranging from -22.5% to -15.3% with an average underestimation of the flow of -18.1%. Only for the Narewka catchment all simulations with the synthetic climate data result in mean flows over the 1976-2005 period that are comparable to the observed mean flow. Deviations between the observed and simulated flows range from -3.5% to +3.5% with an average deviation between the observations and the simulations of -0.6%.

4.5.2 CLIMATE CHANGE IMPACT ON THE TOTAL RUNOFF

Below, in Figure 4-10, the modelled mean annual flows are presented for the Biała Tarnowska, Dunajec and Narewka catchments for the entire sample period of 1971-2100. Each coloured dot represents a GCM/RCM combination and the black line is the median of the seven GCM/RCM combinations. The median value from the ensemble is used to identify changes in the annual total runoff for the catchments. In all three catchments an upward trend is detected indicating an increase in the mean annual flows. These trends are consistent with Osuch et al. (2016) who also identified an upward trend in the annual runoff from various Polish catchments, including the catchments considered in this research. The severity of the changes for each GCM/RCM combination are presented in Table 4-10 as the percentage increase per year over the 1971-2100 period. The calculated upward trend is presented as the average percentage increase per year in the mean annual flow over the 1971-2100 period. The biggest upward trend is observed in the Narewka catchment where an average increase of 0.23% per year is observed in the annual runoff.

The upward trend is explained by the projected changes in the climatic variables that are discussed in section 2.3. For all three catchments both the precipitation and the temperature are projected to increase. Using the future temperature projections, the potential evapotranspiration is calculated. Combining the projected potential evapotranspiration and the precipitation it is shown that the surplus of precipitation increases. This means that the overall wetness of the catchments is projected to increase and therefore also the total runoff from the three catchments. This finding on an increase of wetness of the catchments is supported by (Meresa et al., 2016).

The largest increases in runoff are observed in the winter and spring periods which is explained by the projected changes in the temperature and the precipitation. In Appendix C the projected changes in temperature and precipitation for the near future and far future periods are displayed in plots for all three catchments relative to the observed temperature and precipitation in the reference period. The largest projected increase in temperature are observed in the winter period for all three catchments. This leads to less accumulation of snow in the catchment and more direct runoff in the winter periods. The largest increases projected increase in precipitation is observed in March, April and May which causes the projected increase in runoff in the spring period. These results correspond to the research of Piniewski et al. (2017) who have shown that the largest rate of change in climate change can be observed in the winter and spring periods.

TABLE 4-10: CHANGES IN PERCENTAGE PER YEAR IN MODELLED ANNUAL RUNOFF OVER THE 1971-2100 PERIOD FOR THE BIAŁA TARNOWSKA, DUNAJEC AND NAREWKA CATCHMENTS

	Biała Tarnowska	Dunajec	Narewka
GCM/RCM 1	0,11%	0,05%	0,31%
GCM/RCM 2	0,21%	0,19%	0,37%
GCM/RCM 3	0,20%	0,15%	0,32%
GCM/RCM 4	0,03%	0,05%	0,18%
GCM/RCM 5	0,05%	0,06%	0,15%
GCM/RCM 6	0,20%	0,01%	0,17%
GCM/RCM 7	0,09%	0,06%	0,21%
GCM/RCM mean	0,11%	0,08%	0,23%

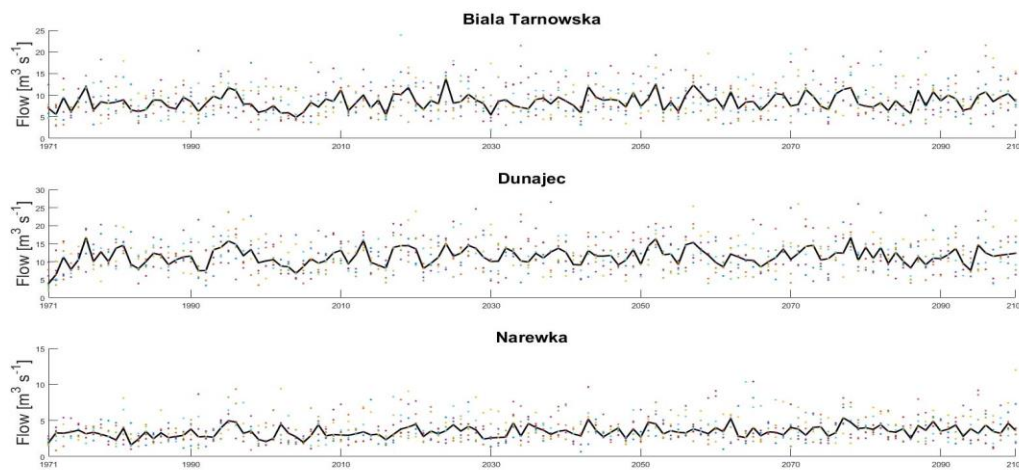


FIGURE 4-10: MODELLED ANNUAL MEAN FLOW FROM THE BIAŁA TARNOWSKA, DUNAJEC AND NAREWKA CATCHMENTS FOR THE 1971-2100 PERIOD

4.5.3 CLIMATE CHANGE IMPACT ON THE RUNOFF COMPONENTS

From the runoff simulations the flow components are derived for the predefined periods. Making use of the Wittenberg filter again, this separation into flow components has been done individually for each of the seven projections generated using the GCM/RCM combinations. The parameters used for the Wittenberg filter are determined individually for each separation. The resulting baseflow indices (BFI) are presented in tables 4-11, 4-12 and 4-13 for the three time periods for each catchment.

TABLE 4-11: DERIVED BFI FOR THE BIAŁA TARNOWSKA CATCHMENT FROM RUNOFF SIMULATIONS FOR EACH OF THE SEVEN GCM/RCM COMBINATIONS FOR THE REFERENCE, NEAR-FUTURE AND FAR-FUTURE PERIOD

	Reference	Near-future	Far-future
GCM/RCM 1	0.63	0.63	0.62
GCM/RCM 2	0.64	0.63	0.63
GCM/RCM 3	0.60	0.60	0.59
GCM/RCM 4	0.61	0.59	0.60
GCM/RCM 5	0.60	0.61	0.59
GCM/RCM 6	0.61	0.61	0.60
GCM/RCM 7	0.61	0.58	0.59
GCM/RCM mean	0.61	0.61	0.60

TABLE 4-12: DERIVED BFI FOR THE DUNAJEC CATCHMENT FROM RUNOFF SIMULATIONS FOR EACH OF THE SEVEN GCM/RCM COMBINATIONS FOR THE REFERENCE, NEAR-FUTURE AND FAR-FUTURE PERIOD

	Reference	Near-future	Far-future
GCM/RCM 1	0.66	0.67	0.66
GCM/RCM 2	0.67	0.66	0.66
GCM/RCM 3	0.65	0.65	0.65
GCM/RCM 4	0.65	0.65	0.65
GCM/RCM 5	0.64	0.64	0.64
GCM/RCM 6	0.66	0.66	0.66
GCM/RCM 7	0.64	0.64	0.65
GCM/RCM mean	0.65	0.65	0.65

TABLE 4-13: DERIVED BFI FOR THE NAREWKA CATCHMENT FROM RUNOFF SIMULATIONS FOR EACH OF THE SEVEN GCM/RCM COMBINATIONS FOR THE REFERENCE, NEAR-FUTURE AND FAR-FUTURE PERIOD

	Reference	Near-future	Far-future
GCM/RCM 1	0.67	0.68	0.67
GCM/RCM 2	0.68	0.67	0.67
GCM/RCM 3	0.66	0.66	0.64
GCM/RCM 4	0.68	0.67	0.66
GCM/RCM 5	0.67	0.66	0.66
GCM/RCM 6	0.67	0.66	0.66
GCM/RCM 7	0.66	0.66	0.67
GCM/RCM mean	0.67	0.67	0.66

It is observed that the GCM/RCM combinations 1 and 2 result in a higher BFI than the other GCM/RCM combinations. Flow projections generated using the GCM/RCM combinations 1 and 2 also display a lower variance in the projected flows compared to the flow projections generated using the other GCM/RCM combinations. This lower variance indicates a more constant flow where less extremes occur and/or runoff extremes are of lower magnitude. As described in section 3.4.1 during runoff events fast runoff gains in contribution whereas the baseflow becomes the

dominant contributor during periods of more constant runoff. Therefore, more runoff events and/or more extreme runoff events would result in a lower BFI which explains why the BFI derived from flow projections using GCM/RCM combinations 1 and 2 is higher than from other GCM/RCM combinations.

It is also observed that, despite the observed differences between the seven simulations, for all three catchments BFI appears to remain stationary between the reference period, the near-future period and the far-future period. Considering this aspect of the runoff from the catchments, projected climate change does not seem to impact the composition of the total runoff from the catchments when assessed on an annual basis.

In tables 4-14, 4-15 and 4-16 the derived BFI's from the seven GCM/RCM combinations are summarized into the mean for each season for each catchment. The seasons are defined as winter (DJF): December, January and February, spring (MAM): March, April and May, summer (JJA): June, July and August and autumn (SON): September, October and November. Full tables in which the results from each of the GCM/RCM combinations are presented in Appendix D.

TABLE 4-14: SEASONAL BFI CONTRIBUTIONS TO THE TOTAL FOW FOR THE BIAŁA TARNOWSKA CATCHMENT FOR THE REFERENCE, NEAR-FUTURE AND FAR-FUTURE PERIODS

	Reference period	Near-future period	Far-future period
DJF	0.68	0.68	0.68
MAM	0.63	0.59	0.59
JJA	0.57	0.57	0.56
SON	0.62	0.63	0.61

TABLE 4-15: SEASONAL BFI CONTRIBUTIONS TO THE TOTAL FOW FOR THE DUNAJEC CATCHMENT FOR THE REFERENCE, NEAR-FUTURE AND FAR-FUTURE PERIODS

	Reference period	Near-future period	Far-future period
DJF	0.74	0.73	0.73
MAM	0.65	0.65	0.65
JJA	0.60	0.61	0.60
SON	0.69	0.69	0.69

TABLE 4-16: SEASONAL BFI CONTRIBUTIONS TO THE TOTAL FOW FOR THE NAREWKA CATCHMENT FOR THE REFERENCE, NEAR-FUTURE AND FAR-FUTURE PERIODS

	Reference period	Near-future period	Far-future period
DJF	0.70	0.69	0.70
MAM	0.66	0.65	0.65
JJA	0.64	0.65	0.63
SON	0.70	0.67	0.68

It is observed that for all catchments the BFI shows interseasonal variability with the BFI being higher during the winter months and lower during the summer period. This seasonal variability in the baseflow is generally attributed to the influence of evapotranspiration leading to a slower flow recession in the winter compared to the summer periods (Gribovski et al., 2014). This means that the runoff peaks are less sharp and thus giving the baseflow component more time to adjust to the total flow (Wittenberg, 2003; Wang & Cai, 2009).

Contribution of the flow components to the total flow is not projected to show large changes in the near-future or far-future compared to the reference period. Wang & Cai (2010) have shown that, by comparing long term changes in baseflow contribution to the total runoff between urban and agricultural catchments, changes in the BFI are primarily induced by human interference. In this research nearly natural catchments are considered (Romanowicz et al., 2016) human interference is not considered in the modelling of future projections. Therefore, it is easily explained that the BFI is not projected to change at both annual and seasonal scales.

4.5.4 PROJECTED CHANGES IN LOW FLOWS

To assess projected changes in low flows the Q90 value is used as performance indicator as described in section 3.5. The Q90 values derived from the reference period of the observations for the considered catchments are presented below in Table 4-17.

TABLE 4-17: Q90 FOR THE BIAŁA TARNOWSKA, DUNAJEC AND NAREWKA CATCHMENTS DERIVED FROM THE OBSERVED RUNOFF FOR THE REFERENCE PERIOD

Catchment	Q90	
Biała Tarnowska	1.90	m ³ s ⁻¹
Dunajec	4.27	m ³ s ⁻¹
Narewka	0.91	m ³ s ⁻¹

For analysing changes in Q90 the mean values of Q90 between the seven GCM/RCM combinations will be used to compare to the Q90 value derived from observations. This choice is made because the Q90 values derived from the simulations displayed a large spread with no clear pattern. The Q90 values that are derived from the simulations for the reference period are presented in Table 4-18.

Comparing the Q90 values for the reference period shows that the average Q90 from the simulated flow is similar to the Q90 from observations for the Biała Tarnowska catchment. The Dunajec and Narewka catchments however display a simulated Q90 that is 9% and 12% lower respectively than the Q90 from observations.

In section 4.5.1 it was already shown that for the reference period the HBV model, forced with synthetic climate data, appeared to underestimate the total runoff generated from the catchments. Therefore, it is not unexpected that the models also underestimate the Q90 for the reference period. In addition to this, multiple researches have shown that because of the model structure of the HBV model, the HBV model is prone to underestimating the low flows (Berglov et al., 2009; Demirel et al., 2013; Tian et al., 2014).

TABLE 4-18: MEAN Q90 FOR THE BIAŁA TARNOWSKA, DUNAJEC AND NAREWKA CATCHMENTS DERIVED FROM THE SIMULATED RUNOFF FOR THE REFERENCE, NEAR-FUTURE AND FAR-FUTURE PERIOD

	Reference		Near-future		Far-future	
Biała Tarnowska	1.90	m ³ s ⁻¹	2.04	m ³ s ⁻¹	2.05	m ³ s ⁻¹
Dunajec	3.90	m ³ s ⁻¹	4.05	m ³ s ⁻¹	4.04	m ³ s ⁻¹
Narewka	0.80	m ³ s ⁻¹	0.96	m ³ s ⁻¹	0.93	m ³ s ⁻¹

To indicate what the impact of climate change might be on the Q90 from the catchments the simulated Q90 derived from the reference period will be compared to the Q90 that is derived from the projected near-future and far-future runoffs. Derived values for the Q90 for the near-future and far-future are also found in table Table 4-18.

The Q90 values for all catchments indicate that between the reference period and the near-future the Q90 values show a similar absolute increase with the Biała Tarnowska Q90 increasing by $0.14 \text{ m}^3 \text{ s}^{-1}$ the Dunajec Q90 increasing by $0.15 \text{ m}^3 \text{ s}^{-1}$ and the Narewka Q90 increasing by $0.16 \text{ m}^3 \text{ s}^{-1}$. Relatively these changes are the largest for the Narewka catchment where an increase of 20% is observed. For the Biała Tarnowska and Dunajec catchments the projected changes to Q90 are an increase of 7.3% and 3.8% respectively. Between the near-future period and the far-future period the Q90 values appear to remain stable and not display large changes despite the climatological variables changing between the periods as was displayed in Appendix C.

5 DISCUSSION

In this chapter it will be reflected on the methodologies applied in this research and the results synthesised by applying the aforementioned methodologies.

5.1 DATASETS

The observed climatological datasets used in this research are obtained from different stations for each catchment, but more notable also a different number of measurement stations per catchment. The datasets containing the climatological variables of the Biała Tarnowska catchment are created from five different measurement stations and combined into one dataset using Thiessen polygons (Knoben, 2013). The datasets of the Dunajec are derived from three measurement stations and the datasets of the Narewka catchment are obtained from one measurement station. This low number of measurement stations used for creating the datasets results in a coarse estimate of the climatological characteristics that are used for the entire catchment. The Narewka catchment is relatively flat and small, so the differences in temperature and precipitation are probably minimal. Using only a single measurement station for the Narewka catchment could be justified. The Biała Tarnowska and Dunajec catchments however are situated in the Carpathian Mountains so orographic effects might influence the variability of precipitation over the catchments and cause a temperature gradient because of altitude differences. Therefore, using a low number of measurement locations might not give the required resolution to generate datasets that accurately resemble the climatological variables of the catchment.

To compensate for this, during model calibration model parameters from the HBV model might have to compensate for these structural errors in PET estimates and errors in precipitation and temperature observations resulting in a suboptimal model parameterisation. This further protrudes in the rest of the study because the obtained model parameterisation is also used for climate change assessment.

5.2 MODEL CALIBRATION

From the sensitivity analysis it was concluded that despite the differences between the catchments several parameters consistently represented most of the variance in the model output. For the NS and the NSL different parameters appear to be the most sensitive parameters. For the sensitivity towards the NS objective function especially parameters related to the fast runoff routine represented most of the model output variance whereas for the NSL the dominant parameters were related to the slow runoff routine which was expected. These results appeared to be mostly consistent among all three catchments giving confidence that the correct parameters are found to which the model output is most sensitive for both objective functions.

For model calibration the SCEM-UA calibration algorithm was used. During the calibration step of the HBV model for all three catchments the SCEM-UA converges to the set of parameter values that supposedly gives the best model outputs according to the NS and NLS objective functions. For the Dunajec and Narewka catchments these parameter sets that are found by the SCEM-UA algorithm display a comparable performance to earlier modelling studies in these catchments (Osuch et al., 2016 and Romanowicz et al., 2016). Comparing the parameter values that are found from the calibration with parameter values from the aforementioned studies it appears that equifinality (Beven & Freer, 2011) poses a problem when using SCEM-UA for model calibration. Despite the parameter sets from the aforementioned studies and the parameter set generated in this study having a comparable performance at simulating the runoff from the catchments the parameter values are different between the parameter sets.

For the Biała Tarnowska catchment SCEM-UA results in a parameter set that performs significantly worse than parameter sets found in the aforementioned studies. Parameter convergence plots show that for all parameters the

model converges to the supposedly optimum solution with parameter ranges similar to those used in earlier studies (e.g. Benninga et al., 2017). Rerunning SCEM-UA with different parameter ranges and different starting points resulted in nearly identical results with a lower NS score than earlier researches have achieved for the calibration period. This artefact has not been dealt with and it was assumed that it would not pose a problem for identifying a relationship between the NS and NSL function weights and the ability to simulate runoff components because the lower scores were consistent for all combinations of function weights.

The HBV model that is used in this research has proven to be able to skilfully simulate runoff from catchments (e.g. Booi, 2005; Benninga et al., 2017; Romanowicz et al. 2016; Kundzewicz et al., 2017). However, the performance of the HBV model is known to be imperfect during periods of low flow (e.g. Berglöv et al., 2009; Tian et al., 2014; Benninga et al., 2017). Demirel et al. (2013) have shown that this increase in uncertainty can be primarily attributed to uncertainty in model parameters and to a lesser extent also to the model inputs. This uncertainty in simulation of low flows however is not exclusive to the HBV model. Tian et al. (2014) have shown that also for the GR4J and Xinanjiang model the uncertainty for low flows is higher than the uncertainty in simulation in high flows. During periods of low flow, the runoff consists (almost) entirely of baseflow so this uncertainty protrudes further into the research when decomposing the total runoff into baseflow and fast runoff where a consistent over- or underestimation of the baseflow could have impacted the BFI that has been determined for each catchment. Using a different (conceptual) hydrological model (e.g. GR4J or Xinanjiang) for modelling the runoff is expected to generate similar results to this research. Correct calibration of the model and finding the most suitable parameter set for the purpose of this research is deemed much more important than the choice of the hydrological model.

Making use of a weighted combination of objective functions for calibration of a hydrological model is a method that has been used before by e.g. Dawdy et al. (1972) who used a combination of the sum of squared log deviations for runoff peaks and the sum of squared log deviations for the estimated surface runoff. More recently Li et al. (2014) employed the Nash-Sutcliffe, R^2 and the Relative Mean error, Lv et al. (2018) used a combination of the pattern correlation coefficient, the root mean squared error, the relative bias and the ratio of the standard deviation and Lv et al. (2018) applied the correlation coefficient and also the root mean squared error. Using a weighted combination of multiple objective functions at variable weight intervals to afterwards determine the optimal combination of function weights appears to be a novel approach in calibration of hydrological models.

In this research the NS and the NSL are used as objective functions which both assess the goodness of the calibration in a similar way with the difference being that the NSL is applied on the log transformed values of the runoff. It can be argued that the similar structure of these two objective functions does not sufficiently display a trade-off between the two functions at simulating the runoff components and that choosing an alternative combination of objective functions would have led to different results from this research. From the results it is concluded that there is a trade-off between the two objective functions regarding a correct simulation of the baseflow component of the runoff but that this trade-off is not so prominent for the correct simulation the fast runoff component. This improvement at simulating at least one of the runoff components at a higher skill indicates that, even though the objective functions display large similarities, they are appropriately chosen. However, this does not exclude other objective functions from being used in a similar approach. For different researches or modelling purposes different predetermined objective functions might improve further on the ability of this calibration concept and generate even better results.

5.3 RESULTS

Identifying a trade-off between using the NS and NSL in model calibration for improving the skill at simulating the individual runoff components was done by executing the calibration at different function weights. In total 11 intervals were used in model calibration, thus resulting in 11 optimal parameter sets. The choice of using only 11

intervals was made based on the time needed to run the SCEM-UA algorithm for all function weight intervals for all three catchments. From these 11 weight intervals a trade-off between the NS and the NSL objective functions could already be identified regarding the correctness at which runoff components are simulated. Increasing the number of intervals at which model calibration will be done is therefore expected not to change the findings from this study, only to increase the certainty in the correlation between the function weight and model skill at simulating the baseflow component.

Projected changes in the total flow seemed to correspond with the findings from previous modelling studies done on Polish catchments including the Biała Tarnowska, Dunajec and Narewka catchments (Meresa et al., 2016; Piniewski et al., 2017). As already stated in paragraph 4.5.2 the overall wetness of the catchments is projected to increase in addition to a projected increase in total annual runoff with the largest increases projected to be in the winter and spring periods. Having similar findings as the two aforementioned studies is not surprising as in this study the same synthetic climate data sets are used as in those previous studies. Reflecting on the results from those studies and the results generated from this study gives confidence in the correctness of model set-up for modelling the runoff from the catchments and the results obtained.

The baseflow contribution to the total flow was calculated by using Wittenberg's baseflow filtering technique. Multi catchment comparison studies have shown that generally, baseflow separation techniques generate comparable results with similar baseflow contributions to the total flow (Eckhardt, 2008; Gonzalez et al. 2009). Therefore, it can be assumed that applying a different baseflow separation technique would not impact the results and conclusions synthesised in this study.

Wittenberg's filter as presented in section 3.4.1 uses two parameters that have to be determined from the receding limbs from the hydrograph. These parameters can be interpreted as characteristics of the catchment describing the runoff response. In this research the two filter parameters have been individually determined for each simulation instead of taking using the parameters that define the runoff recession from observations. Changes in catchment characteristics are not taken into account for modelling future runoff from the catchments so it can be argued that the filter parameters derived from the observed runoff should be applied for assessing all time frames. However, it is uncertain if the runoff response from the catchments will remain the same when the catchments are exposed to different climatological conditions. The influence that the decision to define different filter parameters for each simulation has had is uncertain, however defining unique parameters for each separation should allow for the most accurate separation of total runoff into the runoff components.

According to Nathan and McMahon (1990) baseflow amounts to approximately 50% of the total runoff but higher contributions are also possible depending on catchments characteristics (Romanowicz, 2010; Beck et al., 2013). For all three catchments for all seven GCM/RCM combinations the annual contribution of the baseflow varied between 0.60 and 0.69. Romanowicz and Osuch (2011) found a BFI of 0.64 for the Narewka catchment for the 1960-2006 period whereas in this study a BFI of 0.67 was found for the Narewka catchment for the 1976-2005 period. This relatively high baseflow contribution to the total runoff according to Nathan and McMahon (1990) is likely to be influenced by the presence of snow in all three of the catchments. Rumsey et al. (2015) have shown that there is a positive correlation between snowmelt and an increased contribution of baseflow to the composition of the total runoff. The method applied for baseflow separation in this research however does not explicitly consider snowmelt contribution to the streamflow but solely relies on the shape of the hydrograph. Quantifying the influence of snowmelt on the runoff composition has not been considered in this research.

6 CONCLUSION

The goal of this research was to establish a relationship between using different objective functions and the HBV model its ability to correctly simulate the individual runoff components. By calibrating the HBV model for varying objective function weights for three Polish catchments it was aimed to indicate whether such relationship exists. Two objective functions were used for this purpose: the Nash-Sutcliffe efficiency criterion (NS) and the logarithmic Nash-Sutcliffe efficiency criterion (NSL). After establishment of the relationship between the objective functions and the HBV model's ability to simulate the runoff components the most suited configuration of objective functions was used to calibrate the HBV model and assess the impact of climate change not only on the total runoff but also on the composition of the total runoff.

By calculating the linear correlation between the objective function weights and the skill at which the runoff components are simulated it has been shown that there is a significant trade-off between using the NS and NSL objective functions in calibration of the HBV model when the objective is to simulate the runoff components at the highest skill. There is a positive linear correlation between the function weight assigned to the NSL and the HBV model its ability to correctly simulate the baseflow component. A significant relationship between the objective function weights and the model its ability to correctly simulate the fast runoff component was only found for the Narewka catchment, but appeared to be absent for the Biała Tarnowska and Dunajec catchments.

Establishment of a relationship between the NSL weight and the ability to correctly simulate the baseflow component has led to a calibration where exclusively the NSL was used as objective function for model calibration. Using the parameter set obtained by calibrating the HBV model with the NSL objective function, climate change simulations were run using projected climate data from 7 different combinations of General Circulation Models (GCM) and Regional Climate Models (RCM) under the RCP4.5 emission scenario. Climate change impacts have been assessed for the near-future (2021-2050) and far-future (2071-2100) periods relative to the reference period (1976-2005). Analysis of the results indicates a projected increase in the overall wetness of the catchments accompanied with an increase, of 0.3% increase per year over the 1971-2100 period, in annual runoff for all three catchments in accordance with the findings of Osuch et al. (2016). The largest projected increases in runoff for the considered catchments are observed in the winter and spring periods which corresponds with the results from earlier research from Piniewski et al. (2017).

For flow decomposition Wittenberg's filter for baseflow separation was used to decompose the total runoff in the baseflow component and fast runoff. In the reference period the baseflow contribution to the total runoff or the Baseflow Index (BFI) varied between 61% (0.61) and 68% (0.68) varying between the catchments and GCM/RCM combinations with the BFI in the Biała Tarnowska being on the lower end of that range and the Dunajec and Narewka on the higher end of that range. Separation of the projected runoff into baseflow and quick runoff for the near-future and far-future periods resulted in similar contributions of the baseflow and quick runoff indicating that the composition of the runoff is not projected to change compared to the reference period.

Changes to low flows specifically are indicated by assessing changes in the total runoff during periods of low flow when the total runoff consists (almost) exclusively of baseflow. By looking at changes in the 90th percentile (Q90) of the total runoff it is shown that similarly to how the total runoff from the catchments increases also the magnitude of the baseflow increases. This change only appears to be apparent when comparing the near-future period to the reference period. Between the near-future and the far-future periods the magnitude of the baseflow the baseflow appears to have stabilized and no further projected changes are observed.

7 RECOMMENDATIONS

In chapter 5 the applied methods and results synthesised from this research have been discussed and conclusions have been presented in chapter 6. For further research on this topic that extends from where this research ended several recommendations will be done.

Decomposition of the total runoff in this research has been done by applying Wittenberg's filter for baseflow separation to the total runoff. Gonzalez et al. (2009) have shown that different filtering techniques have little impact on the runoff separation but that the results are inferior to flow decomposition based on tracer data. To accommodate to this limitation that digital filters for flow separation have tracer data can be used to calibrate the filter parameters. For the catchments considered in this research such tracer data was not available. Verifying the results and conclusions drawn from this research can be done in further research by picking catchments that, in addition to runoff and climatological observations, also have records of tracer data.

For runoff separation using Wittenberg's filter, unique filter parameters were determined for each simulation. This was done because it is uncertain if the catchment characteristics that are represented by these filter parameters remain stationary. Investigating how the filter parameters behave under varying conditions can provide the required insights to make a more substantiated choice on how to handle runoff separation for future periods. This should then allow for a more accurate decomposition of the projected runoff and assessment of the impact of climate change of runoff components when catchments are exposed to the projected climatological conditions.

For comparing model performance at simulating the flow components and identifying trade-offs between objective functions for this purpose the Nash-Sutcliffe (NS) and logarithmic Nash-Sutcliffe (NSL) objective functions are used. The results from this research indicated that there was a correlation between the NSL and the skill at which the HBV model simulates the baseflow component. A relationship between an objective function and the skill at which the HBV model simulates the fast runoff component was not found. In further research, to make a more comprehensive comparison, it is advised to incorporate more or different objective functions in the comparison while also dedicating time to find a relationship between an objective function and the ability to simulate the fast runoff component therefore is a worthwhile endeavour.

The research methodologies are applied to three Polish catchments and therefore also the results are limited to a relatively small geographic region. Similarities between the results from the three catchments have been observed where for all three catchments using the NSL allows for the best simulation of the baseflow component. While the results provide valuable insights in how models can be tailored towards simulating runoff components it is uncertain whether the results also hold for catchments with different characteristics. Because of this uncertainty, extrapolating the results conjured from this research to other catchments with different runoff regimes and driving hydrological processes is discouraged. Further research could indicate whether the results from this research can be generalized and extended to a wider variety of catchments with different runoff regimes or within different climatological regions.

8 REFERENCES

- Aksoy, H., Unal, N. E., & Pektas, A. O. (2008). Smoothed minimal baseflow separation tool for perennial and intermittent streams. *Hydrological Processes*, 22, 4467-4476.
- Alkaeed, O., Flores, C., Jino, K., & Tsutsumi, A. (2006). Comparison of Several Reference Evapotranspiration Methods for Itoshima Peninsula Area, Fukuoka, Japan. *Memoirs of the Faculty of Engineering, Kyushu University*, 66.
- Al-Safi, H. I., & Sarukkalige, P. R. (2017). Assessment of future climate change impacts on hydrological behavior of Richmond River Catchment. *Water Science and Engineering*, 10, 197-208.
- Arnold, J. G., & Allen, P. M. (2007). Automated methods for estimating baseflow and groundwater recharge from streamflow records. *Journal of the American Water Resources Association*, 35, 411-424.
- Arnold, J. G., Allen, P. M., Muttiah, R., & Bernhardt, G. (1995). Automated base flow separation and recession analysis techniques. *Groundwater* 33, 1010-1018.
- Bastidas, L. A., Gupta, H. V., Sorooshian, S., Shuttleworth, W. J., & Yang, Z. L. (1999). Sensitivity analysis of a land surface scheme using multicriteria methods. *Journal of Geophysical Research* 104, 19481-19490.
- Beck, H. E., van Dijk, A. I., Miralles, D. G., de Jeu, R. A., Bruijnzeel, L. A., McVicar, T. R., & Schellekens, J. (2013). Global patterns in base flow index and recession based on streamflow observations from 3394 catchments. *Water Resources Research*, 49, 7843-7863.
- Benninga, H. F., Booij, M. J., Romanowicz, R. J., & Rientjes, T. H. (2017). Performance and limitations of ensemble river flow forecasts. *Hydrology and Earth System Sciences*, 21, 5273-5291.
- Berglöv, G., German, J., Gustavsson, H., Harbman, U., & Johansson, B. (2009). *Improvement HBV model Rhine in FEWS: Final Report*.
- Bergström, S. (1992). *The HBV model - Its structure and applications*. SMHI.
- Bergström, S., & Forsman, A. (1973). Development of a conceptual deterministic rainfall-runoff model. *Hydrology Research*, 4, 144-170.
- Bergström, S., & Lindström, G. (2015). Interpretation of runoff processes in hydrological modelling-experience from the HBV-approach. *Hydrological Processes* 29, 3535-3545.
- Beven, K. (1989). Changing ideas in hydrology: the case of physically-based models. *Journal of Hydrology*, 105, 157-172.
- Beven, K. (2012). *Rainfall-Runoff Modelling: The Primer*. Chichester: Wiley & Sons, Ltd.
- Beven, K., & Freer, J. (2011). Equifinality, data assimilation, and uncertainty estimation in mechanistic modelling of complex environmental systems using the GLUE methodology. *Journal of Hydrology*, 249, 11-29.
- Bisterbosch, J. (2010). *Impacts of climate change on low flows in the Rhine basin*. Enschede: University of Twente.
- Blume, T., Zehe, E., & Bronstert, A. (2007). Rainfall-runoff response, event-based runoff coefficients and hydrograph separation. *Hydrological Sciences* 52, 843-862.

- Booij, M. J. (2005). Impact of climate change on river flooding assessed with different spatial model resolutions. *Journal of Hydrology* 303, 176-198.
- Chapman, T. (1999). A comparison of algorithms for stream flow recession and baseflow separation. *Hydrological Processes*, 13, 701-714.
- Cheng, Q. (2014). *Evaluating the Effect of Objective Functions on Model Calibration*. Berlin: Freie Universität Berlin.
- CHIHE. (2016). *Research outline*. Retrieved December 14, 2017, from CHIHE: Climate Change Impact on Hydrological Extremes: <http://chihe.igf.edu.pl/index.php/research-outline>
- Collischonn, W., & Fan, F. M. (2013). Defining Parameters for Eckhardt's Digital Baseflow Filter. *Hydrological Processes* 27, 2614-2622.
- Core Writing Team, Pachauri, R. K., & Meyer, L. A. (2014). *Climate Change 2014: Synthesis Report*. Geneva: IPCC.
- Dawdy, D. R., Lichty, R. W., & Bergmann, J. M. (1972). *A Rainfall-Runoff Simulation Model for Estimation of Flood Peaks for Small Drainage Basins*. Washington D.C.: United States Government Printing Office.
- Demirel, M. C., Booij, M. J., & Hoekstra, A. Y. (2013). Effect of different uncertainty sources on the skill of 10 day ensemble low flow forecasts for two hydrological models. *Water resources research*, 49, 4035-4053.
- Duan, Q., Gupta, V. K., & Sorooshian, S. (1992). Effective and efficient global optimization for conceptual rainfall-runoff models. *Water Resources Research* 28, 1015-1031.
- Eckhardt, K. (2005). How to Construct Recursive Digital Filters for Base Flow Separation. *Hydrological Processes* 19, 507-515.
- Eckhardt, K. (2008). A comparison of baseflow indices, which were calculated with seven different baseflow separation methods. *Journal of Hydrology*, 352, 168-173.
- Eckhardt, K., Haverkamp, S., Fohrer, N., & Frede, H. G. (2002). SWAT-G, a version of SWAT92.2 Modified for Application to Low Mountain Range Catchments. *Physics and Chemistry of the Earth* 27, 641-644.
- Federer, C. A. (1973). Forest transpiration greatly speeds up streamflow recession. *Water Resources Research*, 9, 1599-1604.
- Fenicia, F., Savenije, H. H., Matgen, P., & Pfister, L. (2006). Is the groundwater reservoir linear? Learning from data in hydrological modelling. *Hydrology and Earth System Sciences*, 10, 139-150.
- Frey, H. C., & Patil, S. R. (2002). Identification and Review of Sensitivity Analysis Methods. *Risk Analysis*, 22, 553-578.
- Gan, R., & Luo, Y. (2013). Using the nonlinear aquifer storage–discharge relationship to simulate the base flow of glacier- and snowmelt-dominated basins in northwest China. *Hydrology and Earth System Sciences*, 17, 3577-3586.
- Gelman, A., & Rubin, D. B. (1992). Inference from iterative simulation using multiple sequences. *Stat. Sci.*, 7, 457-472.
- Gonzales, A. L., Nonner, J., Heijkers, J., & Uhlenbrook, S. (2009). Comparison of Different Base Flow Separation Methods in a Lowland Catchment. *Hydrology and Earth Systems Sciences*, 13, 2055-2068.

- Gorgen, K., Beersma, J., Brahmer, G., Buitenveld, H., Carambia, M., de Keizer, O., . . . Volken, D. (2010). *Assessment of climate change impacts on discharge in the Rhine river basin: Results of the RheinBlick2050 project*. CHR.
- Gribovski, Z., Kalicz, P., Kucsara, M., Szilágyi, J., & Vig, P. (2014). Evapotranspiration calculation on the basis of riparian zone water balance. *Acta Silv. Lign. Hung.*, 4, 95-106.
- Hamon, W. R. (1961). Estimating potential evapotranspiration. *Journal of Hydraulics Division*, 87, 107-120.
- Hatterman, F. F., Vetter, T., Breur, L., Su, B., Daggupati, P., Donnelly, C., . . . Krysanova, V. (2017). Sources of uncertainty in hydrological climate impact assessment: a cross-scale study. *Environmental Research Letters*, 13.
- Homma, T., & Saltelli, A. (1996). Importance measures in global sensitivity analysis of nonlinear models. *Reliability Engineering and System Safety* 52, 1-17.
- IPCC. (2013). *Climate Change 2013: The Physical Science Basis. Contribution of Working Group I to the Fifth Assessment Report of the Intergovernmental Panel on Climate Change*. Cambridge, United Kingdom: Cambridge University Press.
- Jajarmizadeh, M., Harun, S., & Salarpour, M. (2012). A Review on Theoretical Consideration and Types of Models in Hydrology. *Journal of Environmental Science and Technology*, 5, 249-261.
- Jedrzejewska, B., & Jedrzejewski, W. (1998). *Predation in Vertebrate Communities*. Warsaw: Mammal Research Institute, Polish Academy of Sciences.
- Klemeš, V. (1986). Operational testing of hydrological simulation models. *Hydrological Sciences Journal* 31, 13-24.
- Knoben, W. J. (2013). *Estimation of non-stationary hydrological model parameters for the Polish Welna catchment*. Enschede: University of Twente.
- Kollat, J. B., Reed, P. M., & Wagener, T. (2012). When are multiobjective calibration trade-offs in hydrologic models meaningful? *Water Resources Research*, 48, 3520-3538.
- Krause, P., Boyle, D. P., & Bäse, F. (2005). Comparison of different efficiency criteria for hydrological model assessment. *Advances in Geosciences*, 5, 89-97.
- Kundzewicz, Z. W., Stoffel, M., Niedzwiedz, T., & Wyzga, B. (2016). *Flood Risk in the Upper Vistula Basin*. Kraków: Springer International Publishing.
- Kundzewicz, Z. W., Stoffel, M., Wyzga, B., Ruiz-Villanueva, V., Niedzwiedz, T., Kaczka, R., . . . Janecka, K. (2017). Changes of flood risk on the northern foothills of the Tatra Mountains. *Acta Geophysica* 65, 799-807.
- Lemons, P. J., & McCray, J. E. (2007). Modeling hydrology in a small Rocky Mountain watershed serving large urban populations. *Journal of the American Water Resources Association*, 43, 875-887.
- Li, H., Beldring, S., Xu, C., & Jain, S. K. (2014). Modelling runoff and its components in Himalayan basins. *Hydrology in a Changing World: Environmental and Human Dimensions*, 363, 158-264.
- Lindström, G., Johansson, B., Persson, M., Gardelin, M., & Bergström, S. (1997). *Development and rest of the distributed HBV-96 Hydrological Model*. Norrköping: Swedish Meteorological Institute.

- Lindström, G., Johansson, B., Persson, M., Gardeling, M., & Bergström, S. (1997). Development and test of the distributed HBV-96 hydrological model. *Journal of Hydrology*, 201, 272-288.
- Linsley, R. K., Kohler, M. A., & Paulhus, J. L. (1975). *Hydrology for Engineers*. McGraw-Hill.
- Lv, M., Lu, H., Yang, K., Xu, Z., Lv, M., & Huang, X. (2018). Assessment of Runoff Components Simulated by GLDAS against UNH-GRDC Dataset at Global and Hemispheric Scales. *Water*, 10, 969-985.
- Marshall, L., Nott, D., & Sharma, A. (2004). A comparative study of Markov chain Monte Carlo methods for conceptual rainfall-runoff modeling. *Water Resources Research*, vol. 40, 2501-2512.
- Meresa, H. K., & Romanowicz, R. J. (2017). *The Critical Role of Uncertainty in Projections of Hydrological Extremes*. Warsaw: Institute of Geophysics Polish Academy of Sciences.
- Meresa, H. K., Osuch, M., & Romanowicz, R. (2016). Hydro-Meteorological Drought Projections into the 21-st Century for Selected Polish Catchments. *Water*, 8, Article Number: 206.
- Merz, R., Parajka, J., & Blöschl, G. (2003). Parameter estimation in distributed hydrological catchment modelling using automatic calibration with multiple objectives. *Advances in Water Resources*, 26, 205-216.
- Metropolis, N., Rosenbluth, A. W., Rosenbluth, M., Teller, A. H., & Teller, E. (1953). Equations of state calculations by fast computing machines. *J. Chem. Phys.*, 21, 1087-1091.
- Napiorkowski, M. J., Piotrowski, A. P., & Napiorkowski, J. J. (2014). Stream temperature forecasting by means of ensemble of neural networks: Importance of input variables and ensemble size. *River Flow 2014*, 2017-2025.
- Nash, J. E., & Sutcliffe, J. V. (1970). River flow forecasting through conceptual models part I - A discussion of principles. *Journal of Hydrology*, 10, 282-290.
- Nathan, R. J., & McMahon, T. A. (1990). Evaluation of Automated Techniques for Base Flow and Recession Analyses. *Water Resources Research* 26, 1465-1473.
- Osuch, M., Lawrence, D., Meresa, H. K., Napiorkowski, J. J., & Romanowicz, R. J. (2017). Projected changes in flood indices in selected catchments in Poland in the 21st century. *Stochastic Environmental Research and Risk Assessment*, 31, 2435-2457.
- Pechlivanidis, I. G., Jackson, B. M., McIntyre, N. R., & Wheeler, H. S. (2011). Catchment scale hydrological modelling :a review of model types, calibration approaches and uncertainty analysis methods in the context of recent developments in technology and applications. *Global Nest Journal* 13, 193-214.
- Perrin, C., Michel, C., & Andréassian, V. (2003). Improvement of a parsimonious model for streamflow simulation. *Journal of Hydrology* 279, 275-289.
- Piniewski, M., Mezghani, A., Szczesniak, M., & Kundzewicz, Z. W. (2017). Regional projections of temperature and precipitation changes: Robustness and uncertainty aspects. *Meteorologische Zeitschrift*, 26, 223-234.
- Romanowicz, R. (2010). An application of a log-transformed low-flow (LTLF) model to baseflow separation. *Hydrological Sciences Journal*, 55, 952-964.

- Romanowicz, R. J., & Osuch, M. (2011). Assessment of land use and water management induced changes in flow regime of the Upper Narew. *Physics and Chemistry of the Earth*, 36, 662-672.
- Romanowicz, R. J., Bogdanowicz, E., Debele, S. E., Doroszkiewicz, J., Hisdal, H., Lawrence, D., . . . Wong, W. (2016). *Climate Change Impact on Hydrological Extremes: Preliminary Results from the Polish-Norwegian Project*. Warsaw: Acta Geophysica.
- Rowinski, P. (2013). *Experimental and Computational Solutions of Hydraulic Problems*. Warsaw: Institute of Geophysics, Polish Academy of Sciences.
- Rumsey, C. A., Miller, M. P., Susong, D. D., Tillman, F. D., & Anning, D. W. (2015). Regional scale estimates of baseflow and factors influencing baseflow in the Upper Colorado River Basin. *Journal of Hydrology: Regional studies*, 4, 91-207.
- Saltelli, A., Tarantola, S., & Campolongo, F. (2000). Sensitivity Analysis as an Ingredient of Modeling. *Statistical Science* 15, 377-395.
- Saltelli, A., Tarantola, S., Campolongo, F., & Ratto, M. (2004). *Sensitivity Analysis in Practice, A Guide to Assessing Scientific Models*. Chichester: John Wiley & Sons Ltd.
- Singh, V. P. (1995). *Computer Models of Watershed Hydrology*. Colorado: Water Resources Publications, 2012.
- SMHI. (2006). *Integrated Hydrological Modelling System (IHMS) Manual Version 5.10*. Norrköping: SMHI.
- Sobol, I. M. (1990). Sensitivity Estimates for Nonlinear Mathematical Models. *Matematicheskoe Modelirovanie*, 2, 407-414.
- Song, X., Zhang, J., Zhan, C., Xuan, Y., Ye, M., & Xu, C. (2015). Global sensitivity analysis in hydrological modeling: Review of concepts, methods, theoretical framework, and applications. *Journal of Hydrology* 523, 739-757.
- Stevenson, A. (2002). *Oxford Dictionary of English* (2nd ed.). Oxford: Oxford University Press.
- Su, N. (1995). The Unit Hydrograph Model for Hydrograph Separation. *Environment International* 21, 509-515.
- Swamy, A. N., & Brivio, P. A. (1997). Modelling runoff using optical satellite remote sensing data in a high mountainous Alpine catchment of Italy. *Hydrological Processes*, 11, 1475-1491.
- Tallasken, L. M. (1995). A review of baseflow recession analysis. *Journal of Hydrology* 165, 349-370.
- Tang, Y., Reed, P., Wagener, T., & Van Werkhoven, K. (2007). Comparing sensitivity analysis methods to advance lumped watershed model identification and evaluation. *Hydrology and Earth System Sciences* 11, 793-817.
- te Linde, A. H., Aerts, J. C., Hurkmans, R. T., & Eberle, M. (2008). Comparing model performance of two rainfall-runoff models in the Rhine basin using different atmospheric forcing data sets. *Hydrology and Earth Systems Sciences*, 943-957.
- Tesemma, Z. K., Wei, Y., Peel, M. C., & Western, A. W. (2014). Effect of year-to-year variability of leaf area index on variable infiltration capacity model performance and simulation of streamflow during drought. *Hydrology and Earth Systems Sciences* 11, 10515-10522.

- Tian, Y., Booij, M. J., & Xu, Y. P. (2014). Uncertainty in high and low flows due to model structure and parameter errors. *Stochastic Environmental Research and Risk Assessment*, *28*, 319-322.
- Tian, Y., Xu, Y., & Zhang, X. (2013). Assessment of Climate Change Impacts on River High Flows through Comparative Use of GR4J, HBV and Xinanjiang Models. *Water Resources Management*, *27*, 2871-2888.
- Vrugt, J. A., Gupta, H. V., Bouten, W., & Sorooshian, S. (2003a). A Shuffled Complex Evolution Metropolis algorithm for optimization and uncertainty assessment of hydrologic model parameters. *Water Resources Research*, *39*, 1-16.
- Vrugt, J. A., Gupta, H. V., Bouten, W., & Sorooshian, S. (2003b). *Shuffled Complex Evolution Metropolis (SCEM-UA) algorithm manual*. Tucson: University of Arizona.
- Wang, D., & Cai, X. (2009). Detecting human interferences to low flows through base flow recession analysis. *Water Resources Research*, *45*, W07426. doi:<https://doi.org/10.1029/2009GL041879>
- Wang, D., & Cai, X. (2010). Comparative study of climate and human impacts on seasonal baseflow in urban and agricultural watersheds. *Geophysical Research Letters*, *37*. doi:<https://doi.org/10.1029/2009WR007819>
- Ward, P. J. (2007). *A coupled climate-hydrological model for Meuse palaeodischarge modelling: set-up and calibration*. Amsterdam: Vrije Universiteit Amsterdam.
- Weisman, R. N. (1977). The effect of evapotranspiration on streamflow recession. *Hydrological Sciences Journal*, *22*, 371-377.
- WHO, JRC, & EEA. (2008). *Impacts of Europe's changing climate*. Copenhagen: EEA.
- Wittenberg, H. (1994). Nonlinear analysis of flow recession curves. *IAHS publication*, *221*, 61-67.
- Wittenberg, H. (1999). Baseflow Recession and Recharge as Nonlinear Storage Processes. *Hydrological Processes* *13*, 715-726.
- Wittenberg, H. (2003). Effects of season and man-made changes on baseflow and flow recession: case studies. *Hydrological Processes*, *17*, 2113-2123.
- Wittenberg, H., & Sivapalan, M. (1999). Watershed Groundwater Balance Estimation Using Streamflow Recession Analysis and Baseflow Separation. *Journal of Hydrology* *219*, 20-33.
- Worqlul, A. W., Dile, Y. T., Ayana, E. K., Jeong, J., Adem, A. A., & Gerik, T. (2018). Impact of Climate Change on Streamflow Hydrology in Headwater Catchments of the Upper Blue Nile Basin, Ethiopia. *Water*, *10*, 120-137.
- Wu, K., & Xu, Y. J. (2006). Evaluation of the applicability of the SWAT model for coastal watersheds in Southeastern Louisiana. *Journal of the American Water Resources Association*, *42*, 1247-1260.
- Xuan, W., Fu, Q., Qin, G., Zhu, C., Pan, S., & Xu, Y. (2018). Hydrological Simulation and Runoff Component Analysis over a Cold Mountainous River Basin in Southwest China. *Water*, *10*, 1705-1720.

9 APPENDICES

A. APPENDIX A

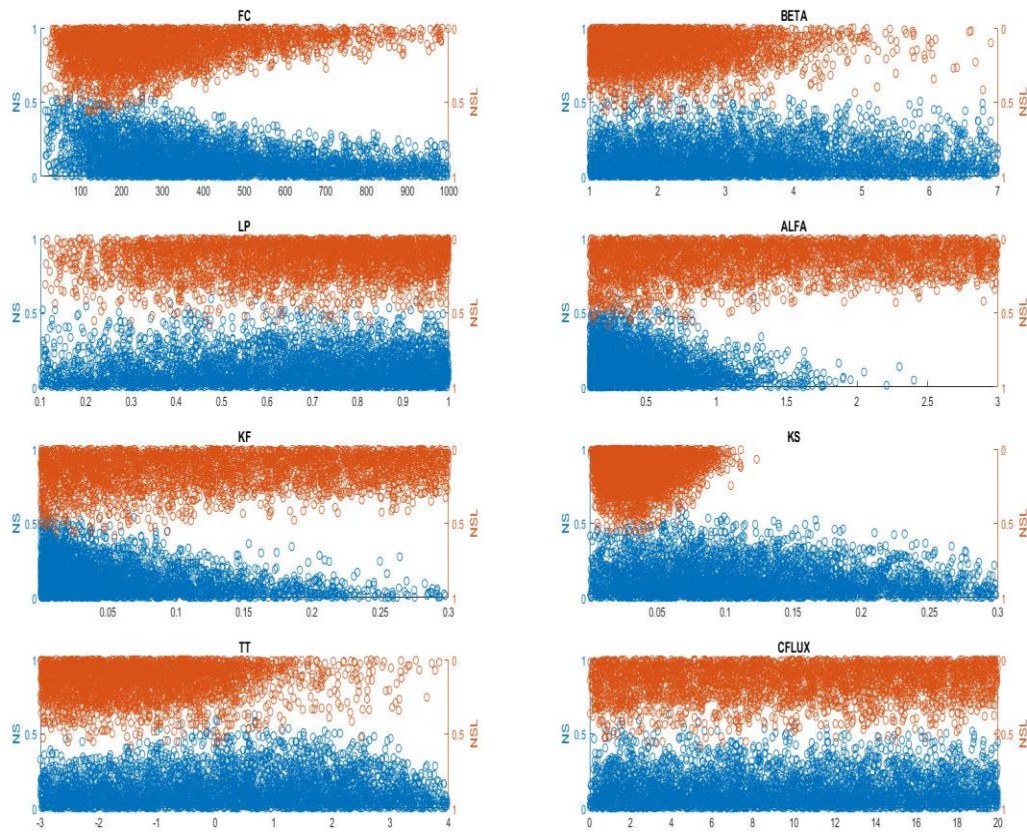


FIGURE A-1: ALL POSITIVE NS AND NSL SCORES PLOTTED AGAINST THE CORRESPONDING PARAMETER VALUE FROM THE MONTE CARLO SIMULATION FOR BIAŁA TARNOWSKA CATCHMENT

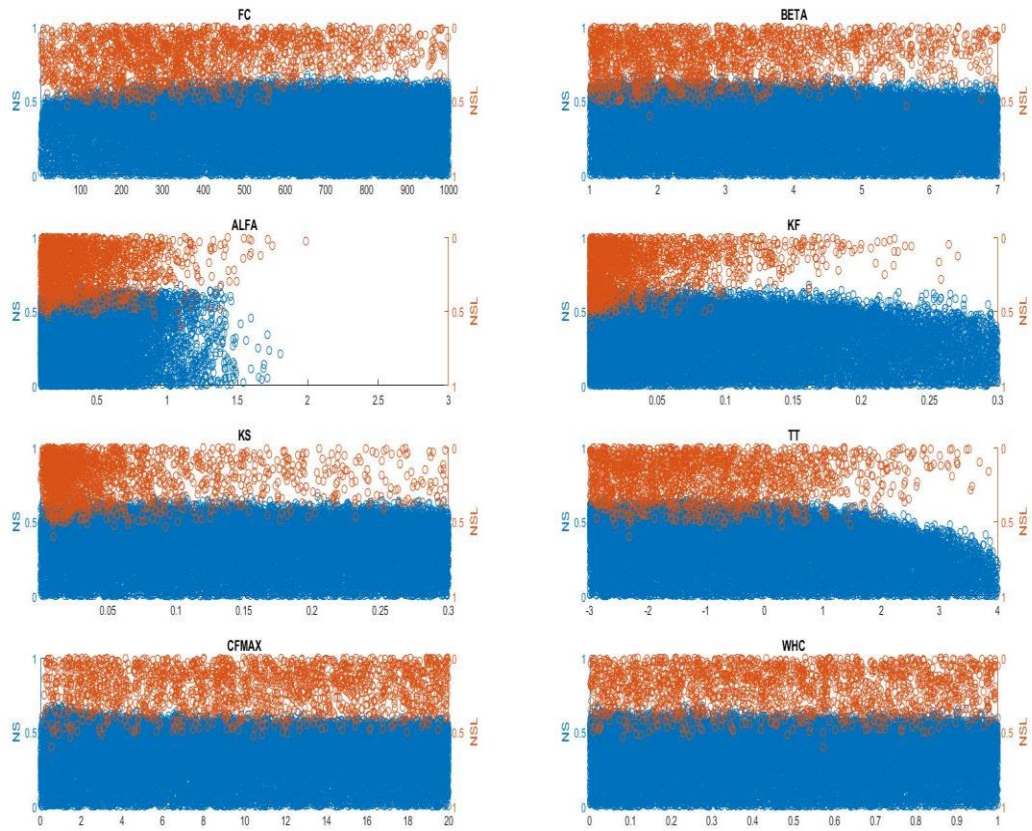


FIGURE A-2: ALL POSITIVE NS AND NSL SCORES PLOTTED AGAINST THE CORRESPONDING PARAMETER VALUE FROM THE MONTE CARLO SIMULATION FOR DUNAJEC CATCHMENT

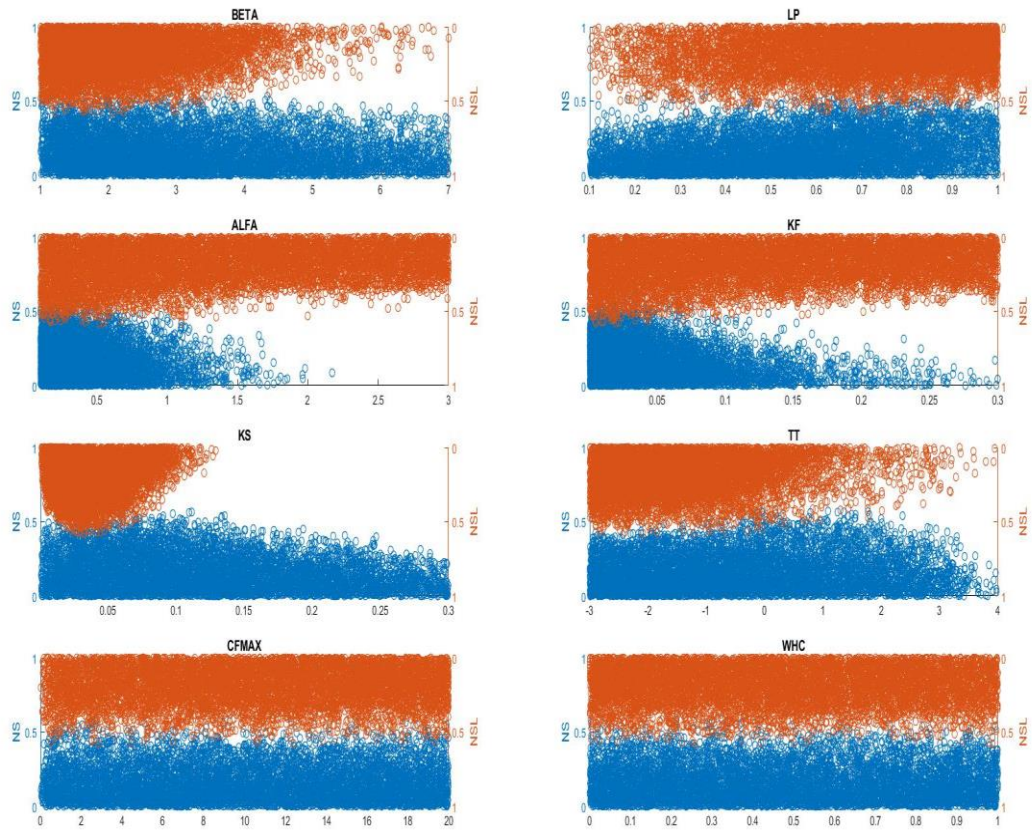


FIGURE A-3: ALL POSITIVE NS AND NSL SCORES PLOTTED AGAINST THE CORRESPONDING PARAMETER VALUE FROM THE MONTE CARLO SIMULATION FOR NAREWKA CATCHMENT

B. APPENDIX B

TABLE B-1: CALIBRATED PARAMETER VALUES FOR THE BIAŁA TARNOWSKA, DUNAJEC AND NAREWKA CATCHMENTS

Parameter	Unit	Biała Tarnowska	Dunajec	Narewka
FC	mm	103	275	200
β	-	2.63	1.53	2.14
LP	-	1	0.23	0.61
α	-	0.40	1.15	0.42
K_f	d ⁻¹	-0.12	0.002	0.03
K_s	d ⁻¹	0.04	0.003	0.04
PERC	mm d ⁻¹	1.6	1.6	1.6
CFLUX	mm d ⁻¹	1	1	1
TT	°C	-0.20	0.10	-0.80
TTI	°C	0	0	0
CFMAX	mm °C ⁻¹ d ⁻¹	0.88	1.66	1.01
FOCFMAX	-	0	0	0
CFR	mm °C ⁻¹ d ⁻¹	0.05	0.05	0.05
WHC	-	0.1	0	0

C. APPENDIX C

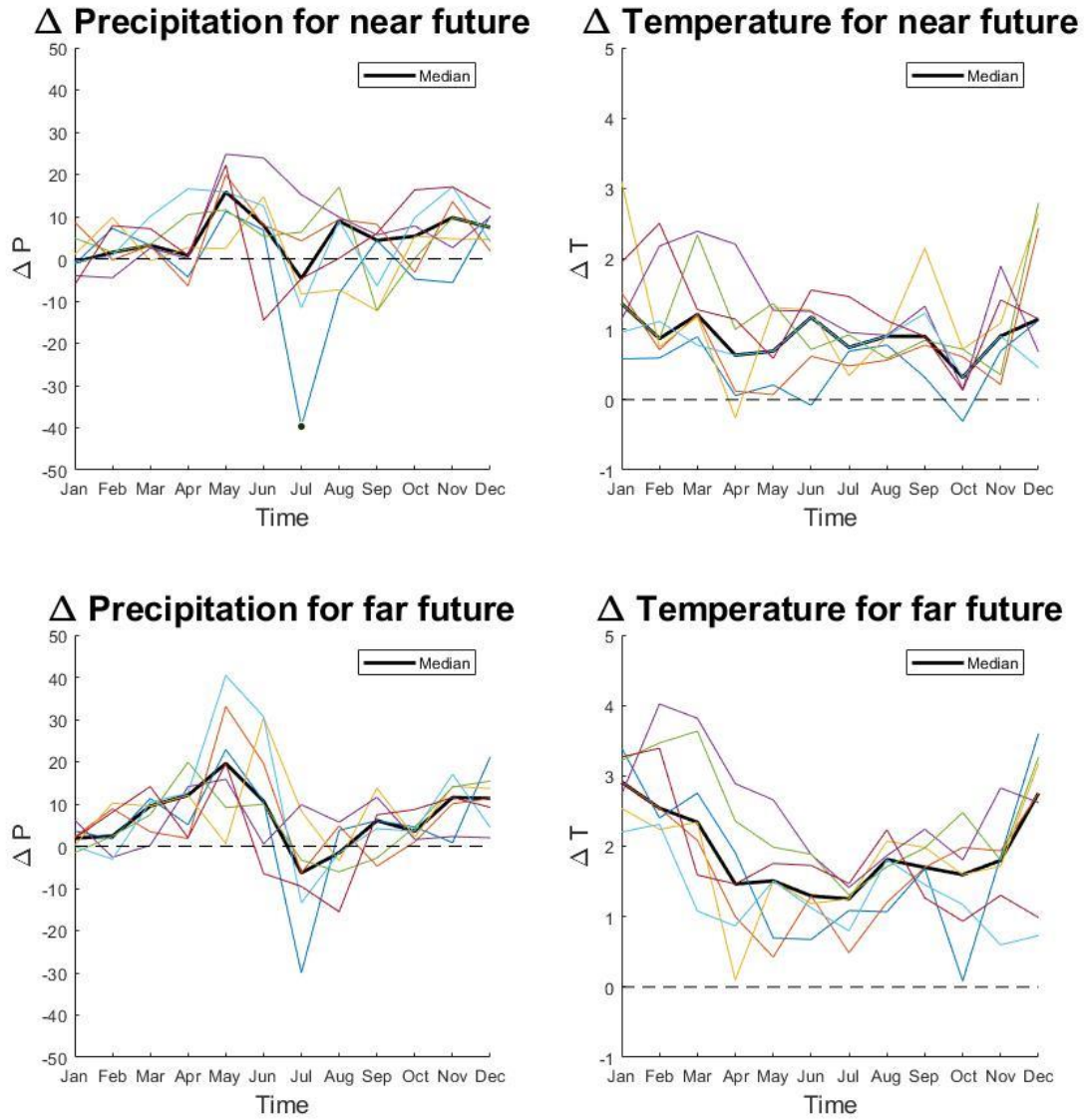


FIGURE C-1: PROJECTED CHANGES IN CLIMATOLOGIC VARIABLES FOR THE NEAR-FUTURE AND FAR-FUTURE FOR THE BIAŁA TARNOWSKA CATCHMENT

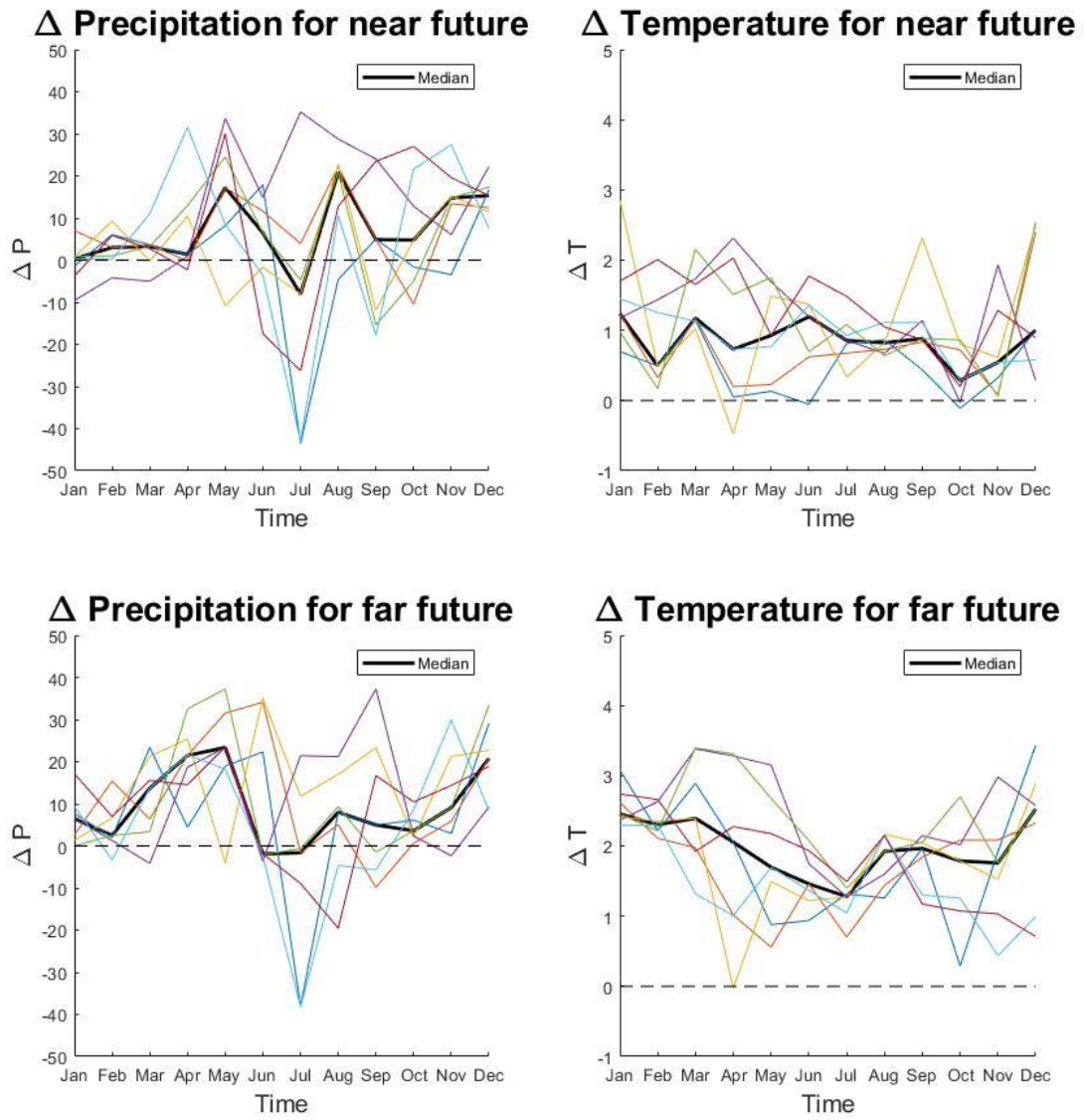


FIGURE C-2: PROJECTED CHANGES IN CLIMATOLOGIC VARIABLES FOR THE NEAR-FUTURE AND FAR-FUTURE FOR THE DUNAJEC CATCHMENT

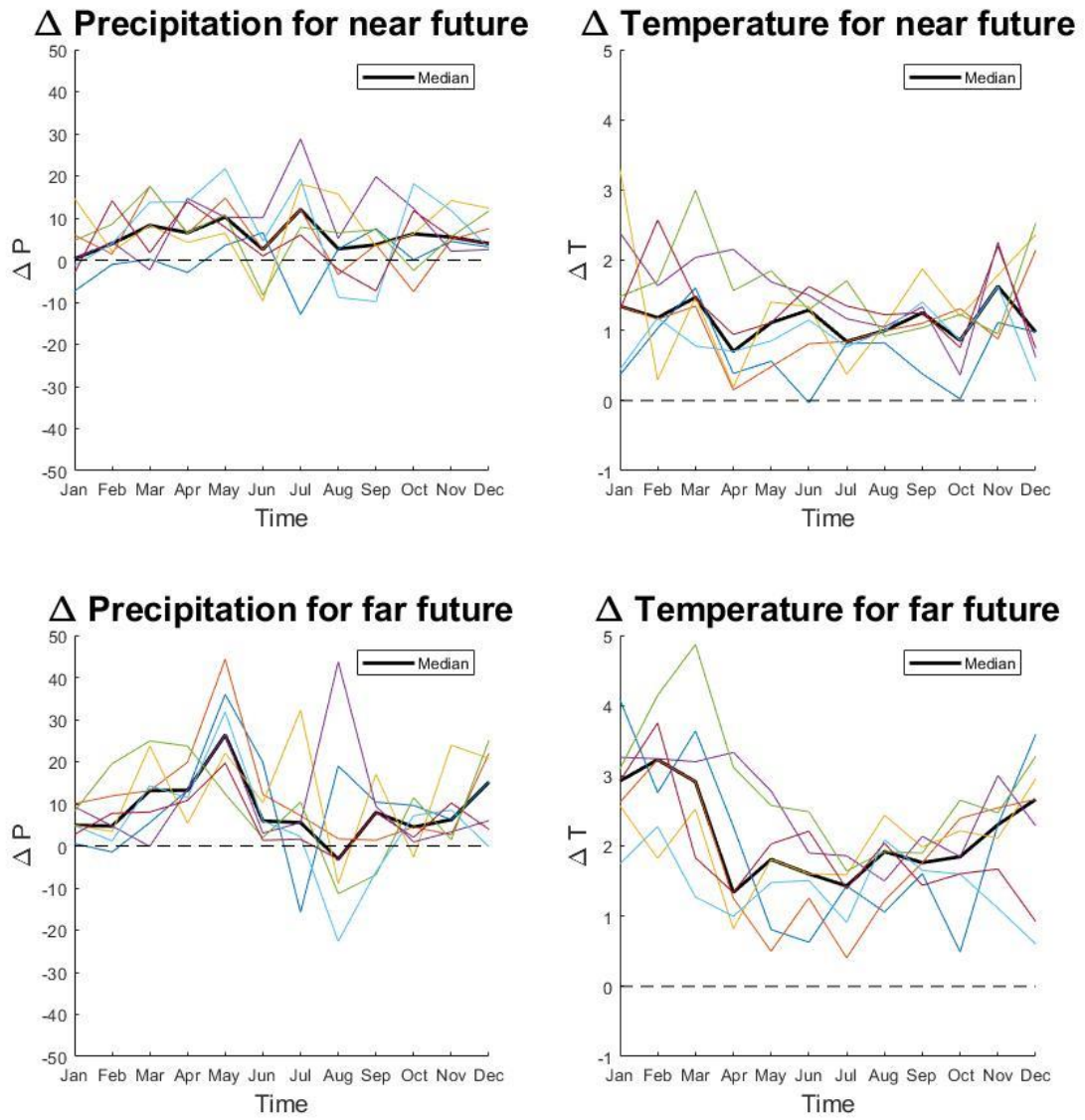


FIGURE C-3: PROJECTED CHANGES IN CLIMATOLOGIC VARIABLES FOR THE NEAR-FUTURE AND FAR-FUTURE FOR THE NAREWKA CATCHMENT

D. APPENDIX D

TABLE D-1: BFI FOR THE WINTER PERIOD FOR THE BIALA TARNOWSKA CATCHMENT

	Reference	Near-future	Far-future
GCM/RCM 1	0.67	0.65	0.65
GCM/RCM 2	0.68	0.67	0.69
GCM/RCM 3	0.69	0.70	0.69
GCM/RCM 4	0.67	0.67	0.66
GCM/RCM 5	0.67	0.66	0.70
GCM/RCM 6	0.69	0.71	0.70
GCM/RCM 7	0.67	0.68	0.67
GCM/RCM mean	0.68	0.68	0.68

TABLE D-2: BFI FOR THE SPRING PERIOD FOR THE BIALA TARNOWSKA CATCHMENT

	Reference	Near-future	Far-future
GCM/RCM 1	0.62	0.60	0.61
GCM/RCM 2	0.65	0.61	0.61
GCM/RCM 3	0.63	0.60	0.64
GCM/RCM 4	0.63	0.60	0.57
GCM/RCM 5	0.63	0.60	0.59
GCM/RCM 6	0.61	0.58	0.55
GCM/RCM 7	0.62	0.56	0.56
GCM/RCM mean	0.63	0.59	0.59

TABLE D-3: BFI FOR THE SUMMER PERIOD FOR THE BIALA TARNOWSKA CATCHMENT

	Reference	Near-future	Far-future
GCM/RCM 1	0.62	0.66	0.62
GCM/RCM 2	0.62	0.61	0.61
GCM/RCM 3	0.54	0.55	0.50
GCM/RCM 4	0.58	0.50	0.58
GCM/RCM 5	0.55	0.57	0.52
GCM/RCM 6	0.54	0.57	0.56
GCM/RCM 7	0.55	0.52	0.53
GCM/RCM mean	0.57	0.57	0.56

TABLE D-4: BFI FOR THE AUTMNM PERIOD FOR THE BIALA TARNOWSKA CATCHMENT

	Reference	Near-future	Far-future
GCM/RCM 1	0.64	0.63	0.60
GCM/RCM 2	0.64	0.63	0.65
GCM/RCM 3	0.60	0.59	0.56
GCM/RCM 4	0.57	0.67	0.60
GCM/RCM 5	0.57	0.64	0.59
GCM/RCM 6	0.65	0.68	0.67
GCM/RCM 7	0.65	0.58	0.61
GCM/RCM mean	0.62	0.63	0.61

TABLE D-5: BFI FOR THE WINTER PERIOD FOR THE DUNAJEC CATCHMENT

DJF	Reference	Near-future	Far-future
GCM/RCM 1	0.75	0.74	0.73
GCM/RCM 2	0.73	0.72	0.73
GCM/RCM 3	0.75	0.73	0.73
GCM/RCM 4	0.73	0.73	0.73
GCM/RCM 5	0.74	0.72	0.75
GCM/RCM 6	0.74	0.74	0.71
GCM/RCM 7	0.73	0.73	0.71
GCM/RCM mean	0.74	0.73	0.73

TABLE D-6: BFI FOR THE SPRING PERIOD FOR THE DUNAJEC CATCHMENT

MAM	Reference	Near-future	Far-future
GCM/RCM 1	0.64	0.65	0.64
GCM/RCM 2	0.66	0.65	0.66
GCM/RCM 3	0.64	0.66	0.67
GCM/RCM 4	0.66	0.68	0.65
GCM/RCM 5	0.66	0.63	0.65
GCM/RCM 6	0.66	0.63	0.65
GCM/RCM 7	0.66	0.62	0.63
GCM/RCM mean	0.65	0.65	0.65

TABLE D-7: BFI FOR THE SUMMER PERIOD FOR THE DUNAJEC CATCHMENT

JJA	Reference	Near-future	Far-future
GCM/RCM 1	0.64	0.64	0.63
GCM/RCM 2	0.63	0.64	0.62
GCM/RCM 3	0.60	0.59	0.59
GCM/RCM 4	0.58	0.57	0.60
GCM/RCM 5	0.57	0.59	0.56
GCM/RCM 6	0.60	0.63	0.63
GCM/RCM 7	0.56	0.60	0.60
GCM/RCM mean	0.60	0.61	0.60

TABLE D-8: BFI FOR THE AUTUMN PERIOD FOR THE DUNAJEC CATCHMENT

SON	Reference	Near-future	Far-future
GCM/RCM 1	0.67	0.70	0.69
GCM/RCM 2	0.69	0.68	0.71
GCM/RCM 3	0.67	0.70	0.67
GCM/RCM 4	0.70	0.69	0.65
GCM/RCM 5	0.67	0.70	0.68
GCM/RCM 6	0.71	0.70	0.71
GCM/RCM 7	0.70	0.66	0.70
GCM/RCM mean	0.69	0.69	0.69

TABLE D-9: BFI FOR THE WINTER PERIOD FOR THE NAREWKA CATCHMENT

DJF	Reference	Near-future	Far-future
GCM/RCM 1	0.70	0.70	0.71
GCM/RCM 2	0.72	0.71	0.70
GCM/RCM 3	0.69	0.70	0.70
GCM/RCM 4	0.70	0.69	0.70
GCM/RCM 5	0.69	0.68	0.68
GCM/RCM 6	0.72	0.71	0.71
GCM/RCM 7	0.69	0.67	0.71
GCM/RCM mean	0.70	0.69	0.70

TABLE D-10: BFI FOR THE SPRING PERIOD FOR THE NAREWKA CATCHMENT

MAM	Reference	Near-future	Far-future
GCM/RCM 1	0.64	0.66	0.65
GCM/RCM 2	0.67	0.63	0.64
GCM/RCM 3	0.66	0.67	0.66
GCM/RCM 4	0.66	0.66	0.68
GCM/RCM 5	0.67	0.64	0.64
GCM/RCM 6	0.68	0.64	0.65
GCM/RCM 7	0.65	0.65	0.65
GCM/RCM mean	0.66	0.65	0.65

TABLE D-11: BFI FOR THE SUMMER PERIOD FOR THE NAREWKA CATCHMENT

JJA	Reference	Near-future	Far-future
GCM/RCM 1	0.67	0.68	0.66
GCM/RCM 2	0.64	0.67	0.67
GCM/RCM 3	0.61	0.62	0.57
GCM/RCM 4	0.66	0.66	0.61
GCM/RCM 5	0.65	0.65	0.63
GCM/RCM 6	0.59	0.65	0.62
GCM/RCM 7	0.64	0.63	0.65
GCM/RCM mean	0.64	0.65	0.63

TABLE D-12: BFI FOR THE AUTUMN PERIOD FOR THE NAREWKA CATCHMENT

SON	Reference	Near-future	Far-future
GCM/RCM 1	0.71	0.67	0.66
GCM/RCM 2	0.71	0.70	0.69
GCM/RCM 3	0.69	0.65	0.64
GCM/RCM 4	0.69	0.66	0.67
GCM/RCM 5	0.70	0.70	0.70
GCM/RCM 6	0.71	0.68	0.69
GCM/RCM 7	0.71	0.67	0.68
GCM/RCM mean	0.70	0.67	0.68

